ISSN 2717-7203

# JOURNAL OF ADVANCES IN MANUFACTURING ENGINEERING

JAME

Volume 7
Number 1
Year 2026 - June

YTÜ PRESS

www.jame.yildiz.edu.tr

ISSN 2717-7203

# JOURNAL OF ADVANCES IN MANUFACTURING ENGINEERING

Volume 7 Number 1 Year 2026 - June

ISSN 2717-7203

# JOURNAL OF ADVANCES IN MANUFACTURING ENGINEERING

JAME

Volume 7 Number 1 Year 2026 - June

**Murat YAZICI**

*Department of Automotive Engineering, Bursa Uludağ University, Bursa, Türkiye*

**Mustafa Cemal ÇAKIR**

*Department of Mechanical Engineering, Bursa Uludağ University, Bursa, Türkiye*

**Navneet KHANNA**

*Institute of Infrastructure Technology Research and Management (IITRAM), India*

**Orhan ÇAKIR**

*Department of Mechanical Engineering, Yıldız Technical University, İstanbul, Turkiye*

**Tolga MERT**

*Department of Mechanical Engineering, Yıldız Technical University, İstanbul, Türkiye*

**Yusuf KAYNAK**

*Department of Mechanical Engineering, Marmara University, İstanbul, Türkiye*

**Abstracting and Indexing:** EBSCO, TÜBİTAK TR Index, Bielefeld Academic Search Engine (BASE), ResearchBible, Open Ukranian Citation Index (OUCI), Scilit, Google, Ideal Online, ASCI, OpenAlex

**Journal Description:** The journal is supported by Yıldız Technical University officially, and is a blind peer-reviewed free open-access journal, published bimontly (June-December).

**Publisher:** Yıldız Technical University

**Editor-in-Chief:** Prof. Alper UYSAL

**Language of Publication:** English

**Frequency:** 2 Issues

**Publication Type:** Online e-version

**Publisher:** Kare Publishing

ISSN 2717-7203

# JOURNAL OF ADVANCES IN MANUFACTURING ENGINEERING

Volume 7 Number 1 Year 2026 - June

## CONTENTS

### Research Articles

Journal of Advances in Manufacturing Engineering
Web page info: https://jame.yildiz.edu.tr
DOI: 10.14744/ytu.jame.2026.00001

Original Article

# Assessment of drilling kinematic configurations and their contribution to surface roughness formation in 40HM+QT steel

**Mateusz BRONIS[1], Mehmet Şükrü ADIN[*2]**

[1]*Department of Machine Design and Machining, Kielce University of Technology, Kielce, Poland*
[2]*Besiri OSB Vocational School, Batman University, Batman, Türkiye*

**ARTICLE INFO**

*Article history*
Received: 04 December 2025
Revised: 26 December 2025
Accepted: 05 January 2026

**Key words:**
ANOVA, CNC, drilling, kinematics, surface roughness.

**ABSTRACT**

The study investigates the influence of three different drilling kinematic systems on the surface roughness (Rt) of holes machined in quenched-and-tempered 40HM (AISI 4140) steel. A full experimental campaign was carried out using a CNC machining center and solid carbide internal-coolant drills. The spindle speed (n), feed per revolution (fn), and drilling kinematics were evaluated using a Taguchi L27 orthogonal array supported by ANOVA and response surface methodology (RSM). The results show that spindle speed is the most influential parameter (46.27% contribution to Rt variability), followed by the kinematic system (34.45%) and feed per revolution (19.28%). The most favorable surface roughness was obtained for the first kinematic system, combining tool rotation with an additional axial oscillation. Higher spindle speeds and a feed of 0.14 mm/rev yielded the lowest Rt values across most configurations. The findings highlight the importance of selecting an appropriate kinematic system, demonstrating that non-standard drilling kinematics can significantly enhance hole quality in heat-treated steels.

**Cite this article as:** Adin, M. Ş., & Bronis, M. (2026). Assessment of drilling kinematic configurations and their contribution to surface roughness formation in 40HM+QT steel. *J Adv Manuf Eng*, 7(1), 1–10.

## INTRODUCTION

Drilling is one of the basic processes of material removal, commonly used in the manufacture of machine parts made of structural steel, tool steel, and difficult-to-machine alloys [1–3]. A particularly important area of research is the drilling of heat-treated steels, which, due to their high hardness, strength, and fatigue resistance, are difficult to machine [4–6]. During the drilling process, hardened and tempered steels generate significant cutting forces, increased temperatures, and intensive tool wear, which directly affects the surface quality of the holes made. One of the key indicators of this quality is surface roughness, which affects dimensional accuracy, joint durability, load-bearing capacity, and the functionality of machine components [7–9].

An important factor influencing the drilling process is the kinematic arrangement, i.e., the distribution of rotational and feed movements between the tool and the workpiece. In a classic system, the tool performs both rotational and feed movements, while in a reverse system, the workpiece rotates [10–12]. In mixed systems, the rotational movement is shared between the tool and the workpiece in different proportions, which changes the dynamic parameters of the process, chip removal, and temperature distribution. These differences directly affect cutting stability, vibration amplitude, and thermal conditions, which in turn influence sur-

***Corresponding author.**
*E-mail address: mehmetsukru.adin@batman.edu.tr

face roughness parameters such as Ra, Rz, and Rt [11, 12]. Despite the importance of kinematic arrangements, most available studies focus on classical drilling, indicating that the topic remains insufficiently explored in the literature. In the available studies on drilling, mathematical models describing surface roughness are rarely found, as emphasized by numerous authors. Balaji, Rao, and Murthy [13] developed a predictive model for the Ra parameter, taking into account the drill tip angle, feed rate, and spindle speed. Kumar and Singh [14] proposed a similar model structure, but included the type of drill bit as an additional factor. Other models presented in the literature, e.g., Kilickap et al. [15], are based only on cutting speed, feed rate, and drilling environment (dry, MQL, air), while Pakistani researchers [16] used a logarithmic approach, describing the Ra parameter as a function of rotational speed, feed rate, and depth of cuts. Ravindranath et al. [17] presented a more comprehensive model, including four input factors: workpiece material, rotational speed, feed rate, and drill coating, achieving an accuracy of 83%. One of the most extensive models was presented by Indian authors [18], who took into account as many as five input parameters – tool type, rotational speed, feed rate, drill diameter, and workpiece material – achieving a high correlation between the model and experimental results, reaching 98%. However, the vast majority of publications focus not on the development of mathematical models, but on the analysis of the impact of individual or several technological parameters on hole roughness. Aamir et al. [19] studied the impact of feed rate and rotational speed, while Italian authors [20] analyzed 3D height and amplitude parameters (Sa, Sq, Ssk, Sku). Khanna et al. [21] assessed the importance of cooling conditions, and German researchers [22] focused on Rz parameters for different tools. Wegert et al. [23] analyzed the Ra, Rz, and Rt parameters depending on the drilling depth, and researchers from India [24] took into account the presence of cooling, feed rate, rotational speed, and hole depth, basing their analysis on an L18 orthogonal table. Subsequent studies concerned, among other things, the optimization of drilling parameters [25, 26], analysis of the influence of drill geometry [27], the influence of rotational speed [28], the impact of feed and cutting speed [29], evaluation of the design of cooling channels, the use of $LN_2$ and $LCO_2$ cryogenic cooling [30], and the influence of tool coatings [31, 32]. In summary, the world literature indicates a large number of studies on the influence of technological parameters on hole roughness, but there are few studies that take into account different kinematic arrangements of the drilling process. There is therefore a need for further exploration of the influence of the kinematic system on surface roughness, especially in the case of heat-treated steels, where machining conditions are particularly demanding. A thorough understanding of these relationships may contribute to the development of more effective machining strategies and improve the quality of holes made in materials with increased hardness.

Recent studies have emphasized that drilling machinability and hole surface quality are strongly influenced not only by cutting parameters, but also by material condition and microstructural modifications resulting from alloying or heat treatment. Güldibi et al. [33] demonstrated that variations in aging conditions significantly affect drilling forces, surface quality, and tool wear in high-strength steels, highlighting the critical role of material state in drilling performance. Similarly, Baysal et al. [34] reported that microstructural refinement induced by rare-earth alloying in aluminum alloys leads to improved surface integrity and reduced thrust force during drilling.

Despite these advances, current literature predominantly focuses on conventional drilling kinematics, while the influence of alternative or non-standard kinematic configurations on surface roughness formation remains insufficiently explored. Therefore, the present study aims to fill this gap by systematically evaluating the effect of different drilling kinematic systems on the Rt surface roughness parameter in heat-treated 40HM (AISI 4140) steel.

## MATERIALS AND METHODS

The material selected for testing was medium-carbon alloy steel 40HM (equivalent to AISI 4140), supplied in a heat-treated state (QT – quenching and tempering). This steel is commonly used in machine components subjected to high variable loads due to its favorable combination of high strength, impact resistance, and wear resistance. The process of hardening followed by tempering stabilizes the mechanical properties of the material and ensures a homogeneous structure with controlled hardness, which is crucial for precision machining. 40HM+QT steel is characterized by increased hardenability resulting from the presence of chromium and molybdenum, which promote the formation of a tempered martensitic-bainitic structure. This structure provides both high strength and adequate fracture resistance, which distinguishes this material from non-alloy structural steels. An additional advantage of 40HM steel is its good machinability compared to other high-strength steels, which is important for turning, drilling, and milling operations. These properties make 40HM steel suitable for manufacturing shafts, gears, pins, bushings, and other components exposed to high operational loads [35, 36]. Figures 1 and 2 depict the percentage chemical composition and properties of heat-treated steel 40HM (equivalent to AISI 4140).

The research was conducted using a machining center equipped with a twelve-position tool head in the VDI30 standard according to DIN 5480, enabling automatic replacement of fixed and rotating tools. The machine has a main spindle with a maximum speed of 5000 rpm, a rated power of 20 kW, and a maximum torque of 2200 Nm, which allows drilling processes to be carried out within a wide range of parameters, including in difficult-to-cut materials.

The design of the center is based on a rigid support frame with optimized geometry, ensuring high resistance to dynamic loads and minimizing vibrations and displacements of the tool-workpiece system. Such structural rigidity is essential for achieving high geometric accuracy and low surface roughness in drilled holes. In addition, the device is equipped with a coolant filtration system that maintains the

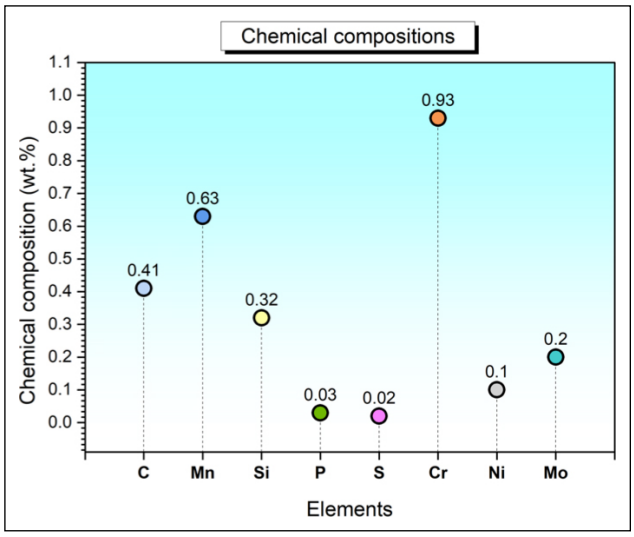


**Figure 1**. Chemical composition of heat-treated 40HM+QT steel.

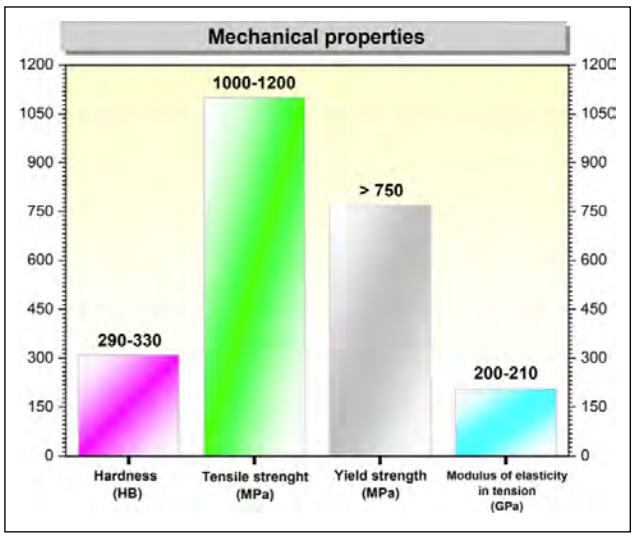


**Figure 2**. Properties of heat-treated steel 40HM+QT.

cleanliness of the machining fluid by effectively removing metal particles, which translates into increased tool life and improved surface quality of machined parts. The "DMG CTX Alpha 500 CNC machine" used in this experimental research is depicted in Figure 3.

In the experimental part, a monolithic drill with a diameter of 6 mm was used, equipped with internal channels supplying coolant directly to the cutting zone. This design promotes effective heat dissipation and efficient chip removal, which in turn reduces tool wear and has a positive effect on the quality of the machined hole surface.

The research included an analysis of three innovative methods of drilling. The first one involved a configuration in which the tool performs the main rotary motion and an additional reciprocating motion along the drilling axis, while the workpiece remains stationary, clamped in the soft jaws of a lathe chuck. A schematic diagram of this method is depicted in Figure 4. This configuration reduces cutting forces, improves chip evacuation, and minimizes adverse

**Figure 3**. View of the DMG CTX alpha 500 CNC machine.

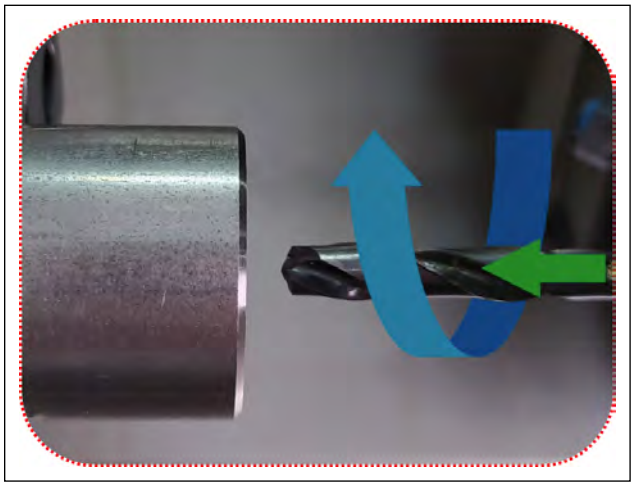

**Figure 4**. First kinematic system.

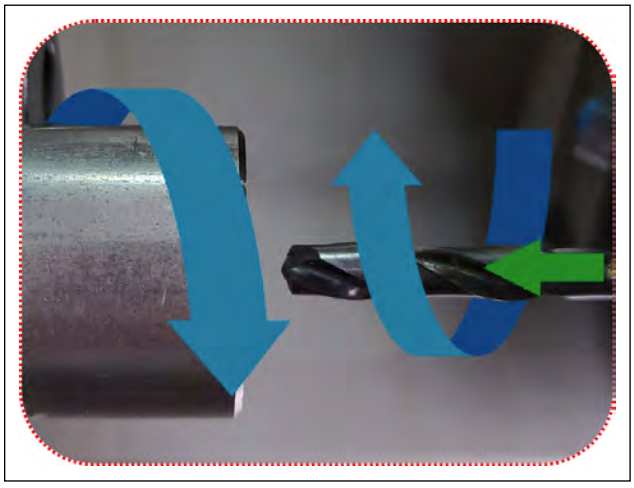

**Figure 5**. Second kinematic system.

effects associated with material expansion during drilling. In addition, the oscillatory motion helps to reduce internal stresses and improves the straightness of the hole.

The second solution analyzed was based on simultaneously setting both the tool and the workpiece in rotational motion, with both elements rotating in opposite directions (Fig. 5). This kinematic arrangement made it possible to

**Table 1.** Drilling process parameters used in the experiments

| Factor | Symbol | Unit | Values |
|---|---|---|---|
| Spindle speed | n | rpm | 3183, 3979, 4775 |
| Feed per revolution | $f_n$ | mm/rev | 0.10, 0.12, 0.14 |
| Kinematic system | KIN | - | I, II, III |
| Drill diameter | D | mm | 6 |
| Point angle of tool | - | ° | 140 |
| Chip flute length | - | mm | 44 |
| Drill type | - | - | Solid carbide, internal coolant |
| Coating | - | - | TiAlNPlus |
| Cooling method | - | - | Flood cooling |
| Workpiece material | - | - | 40HM (AISI 4140) + QT |

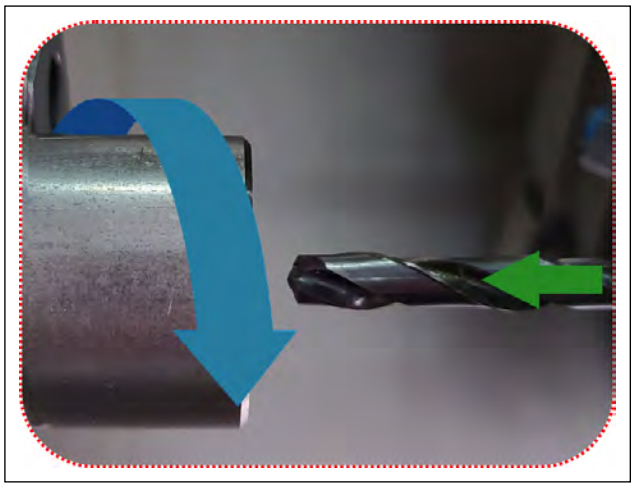

**Figure 6**. Third kinematic system.

achieve a total rotational speed corresponding to the values used in the first and third test configurations.

The use of counter-rotating movements leads to an increase in cutting speed in the tool-material contact area, which can contribute to the intensification of the stock removal process and reduce the formation of build-up on the cutting edge. Additionally, this motion configuration has been shown to reduce axial forces and improve geometric hole parameters of drilled holes, in particular their straightness and surface roughness.

This variant is an example of a non-standard approach to machining, in which the modification of the process kinematics allows for the optimization of cutting parameters and improvement of the quality of the results obtained.

The third drilling concept analyzed was based on a classic kinematic arrangement, in which the tool remains stationary in terms of rotational movement and only performs axial feed along the drilling direction, while the main rotational movement is performed by the workpiece (Fig. 6). This type of configuration is commonly used in traditional drilling operations, both on conventional and numerically controlled (CNC) lathes. In this system, the drill is mounted in a stationary holder, and the rotation of the workpiece results from the operation of the machine spindle. This configuration ensures high concentricity and repeatability of hole geometry, particularly in rotationally symmetrical components, and with appropriately selected feed and cooling parameters, it ensures efficient chip removal.

A set of combinations of various input parameters was created to carry out the experimental work (n = 3183; 3979; 4775 rpm, $f_n$ = 0.1; 0.12; 0.14 mm/rev, KIN I, KIN II, KIN III). The kinematic system was recorded as equation (1) containing the resultant rotational speed of the cutting process.

$$KIN=n_n-n \quad (1)$$

where: KIN – kinematic system $n_n$ – tool rotational speed, n – spindle rotational speed

To systematically investigate the influence of drilling parameters and kinematic configuration on surface roughness (Rt), the Taguchi design of experiments (DOE) method was employed. The Taguchi approach enables efficient evaluation of multiple control factors with a reduced number of experiments while maintaining statistical robustness.

In this experimental research, three control factors were selected: spindle speed (n), feed per revolution ($f_n$), and drilling kinematic system (KIN). Each factor was examined at three levels, resulting in a Taguchi L27 ($3^3$) orthogonal array. This design allows for the assessment of both main effects and interactions between parameters while minimizing experimental effort.

Table 1 summarizes the main drilling parameters and technological conditions applied in the experimental study. These parameters were selected based on tool manufacturer recommendations, preliminary trials, and machine tool limitations.

The selected spindle speed and feed per revolution levels were determined based on tool manufacturer recommendations for drilling heat-treated alloy steels, preliminary trial cuts, and the operational limits of the CNC machining center. The adopted parameter ranges ensured stable cutting conditions without excessive tool wear, chatter, or thermal damage while allowing a clear differentiation of surface roughness responses. The three kinematic systems were chosen to represent fundamentally different drilling motion configurations, including non-standard kinematic solutions, enabling a direct comparison of their influence on surface roughness formation under identical cutting conditions.

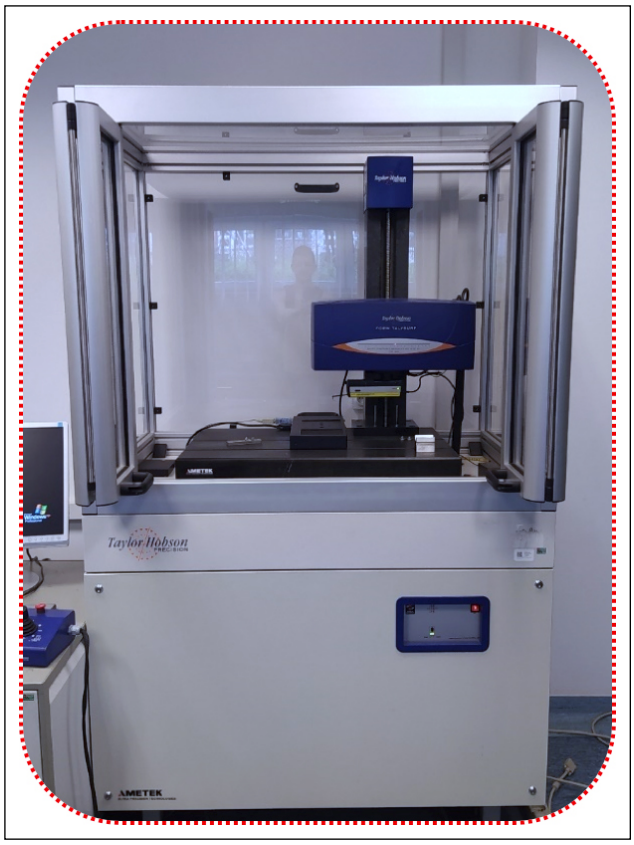


**Figure 7**. View of the Taylor Hobson Form Talysurf PGI 1230 contact profilometer used to measure hole surface roughness (Rt) in 40HM+QT. Measurements were taken on the internal sidewall at mid-depth.

In this experimental research, surface roughness was determined using a Taylor Hobson Form Talysurf PGI 1230 contact profilometer (Fig. 7). The device used ensures high measurement accuracy and repeatability of the results obtained.

The design of experiments (DOE) approach was then applied, using an orthogonal L27 matrix in accordance with the Taguchi method. This allowed for the simultaneous evaluation of the influence of spindle speed (n), feed per revolution ($f_n$), and kinematic drilling variant as input factors on surface roughness (Rt) as a response. A multi-factor analysis of variance (ANOVA) was performed to determine the significance of individual parameters and their interactions. The approach used made it possible to reduce the number of necessary trials while maintaining statistical reliability, providing a solid basis for identifying the key factors affecting the quality of the holes made.

## RESULTS AND DISCUSSION

Table 2 depicts the experimental results obtained within the scope of this research. The following results are presented in relation to the roughness Rt of the 40HM+QT samples. The study utilized a total of 27 samples.

The experimental results revealed a significant variation in the Rt surface roughness values depending on the drilling parameters and kinematic configuration. The lowest Rt value of 2.222 µm was obtained for the first kinematic system (KIN I) at a spindle speed of 4775 rpm and a feed of 0.14 mm/rev, whereas the highest Rt value reached 4.574 µm for the third kinematic system (KIN III) at 3979 rpm and a feed of 0.12 mm/rev. This corresponds to an increase in surface roughness of approximately 106%, indicating a substantial deterioration in surface quality when unfavorable kinematic and cutting conditions are applied. On average, the use of the first kinematic system resulted in Rt values that were approximately 30–45% lower compared to the second and third kinematic configurations, confirming the beneficial effect of superimposed axial oscillation on surface quality. The Rt values obtained within the scope of this experimental research are depicted in Figure 8.

Analysis of variance (ANOVA) was performed using the response surface method (RSM), which is a structured approach to modeling and optimizing process results depending on input variables (Table 3). This method combines the features of polynomial regression, which describes the vari-

**Table 2.** Experimental results

| *Trial* | *n*, rpm | $f_n$, mm/rev | KIN, rpm | Rt, µm |
|---|---|---|---|---|
| 1 | 4775 | 0.14 | 4775 | 2.222 |
| 2 | 4775 | 0.14 | -4775 | 3.698 |
| 3 | 4775 | 0.14 | 0 | 3.806 |
| 4 | 3979 | 0.14 | 3979 | 3.835 |
| 5 | 3979 | 0.14 | -3979 | 4.138 |
| 6 | 3979 | 0.14 | 0 | 4.336 |
| 7 | 3183 | 0.14 | 3183 | 3.711 |
| 8 | 3183 | 0.14 | -3183 | 3.822 |
| 9 | 3183 | 0.14 | 0 | 4.254 |
| 10 | 4775 | 0.12 | 4775 | 3.594 |
| 11 | 4775 | 0.12 | -4775 | 4.38 |
| 12 | 4775 | 0.12 | 0 | 4.003 |
| 13 | 3979 | 0.12 | 3979 | 3.987 |
| 14 | 3979 | 0.12 | -3979 | 4.254 |
| 15 | 3979 | 0.12 | 0 | 4.574 |
| 16 | 3183 | 0.12 | 3183 | 4.054 |
| 17 | 3183 | 0.12 | -3183 | 4.107 |
| 18 | 3183 | 0.12 | 0 | 3.945 |
| 19 | 4775 | 0.1 | 4775 | 3.924 |
| 20 | 4775 | 0.1 | -4775 | 4.215 |
| 21 | 4775 | 0.1 | 0 | 4.209 |
| 22 | 3979 | 0.1 | 3979 | 4.277 |
| 23 | 3979 | 0.1 | -3979 | 4.116 |
| 24 | 3979 | 0.1 | 0 | 4.235 |
| 25 | 3183 | 0.1 | 3183 | 4.152 |
| 26 | 3183 | 0.1 | -3183 | 4.371 |
| 27 | 3183 | 0.1 | 0 | 4.006 |

KIN: Kinematic system.

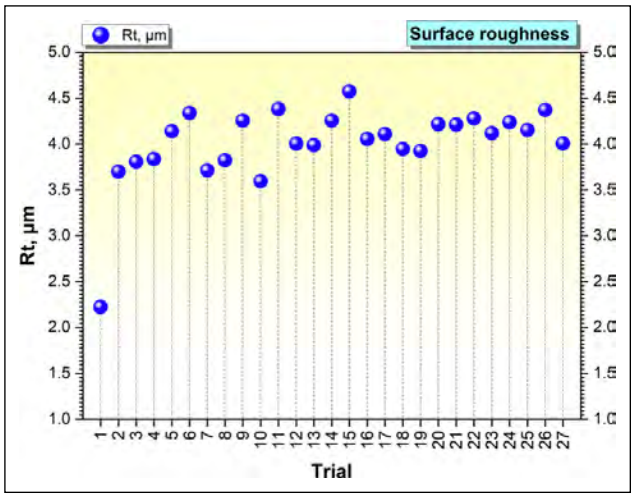


**Figure 8**. Rt values obtained within the scope of this experimental research.

ability of the response as a function of the numerical values of independent variables, and factorial regression, which is characteristic of classical experimental designs. The response surface regression model allows for both linear and nonlinear (quadratic) effects, as well as interactions between factors. The generalized form of the model for two independent variables is represented by the following equation (2):

$$Y=b_0+b_1 X_1+b_2 X_2+b_3 X_1^2+b_4 X_2^2+b_5 X_1 X_2 \quad (2)$$

where:

– y – the value of the response variable (e.g. Rt),

– $b_0$ – free expression,

– $b_1$, $b^2$ – linear regression coefficients,

– $b_3$, $b_4$ – quadratic regression coefficients,

– $b_5$ – interaction coefficient between variables.

In the context of this experimental research, the contribution rates obtained as a result of the ANOVA analysis are depicted in Figure 9.

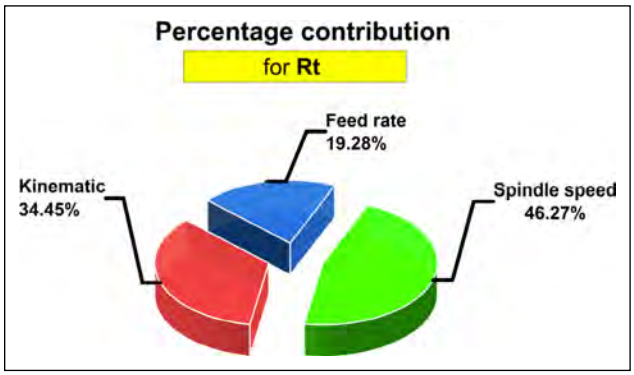


**Figure 9**. Percentage contribution for Rt.

Figure 9 depicts that spindle speed accounted for 46.27% of the variation in the Rt parameter. The kinematic system had an impact of 34.45%, while the rest was attributable to the feed per revolution (19.28%).

In analyzing kinematic system (equation 3),

$$Rt_{40HM}=-10.44+4.52\cdot10^{-3}\cdot n-4.31\cdot10^{-7}\cdot n^2+ +111.22\cdot f_n-342.91\cdot f_n^2+3.77\cdot10^{-4}\cdot KIN+ -1.42\cdot10^{-8}\cdot KIN^2-9.84\cdot10^{-3}\cdot n\cdot f_n-4.99\cdot10^{-8}\cdot n\cdot KIN+ -1.83\cdot10^{-3}\cdot f_n\cdot KIN \quad (3)$$

where: n – spindle speed value, $f_n$ – feed rate per revolution, KIN – kinematics, $n\cdot f_n$ – interaction of spindle speed value with feed rate per revolution, n· KIN – interaction of spindle speed value with kinematics, $f_n$· KIN – interaction of feed rate per revolution with kinematics. As seen in Figure 10, the main effects plot is depicted.

The data presented in Figure 10 depicts that using a rotational speed of 4775 rpm, the lowest Rt parameter value of 3.783 µm was obtained, which corresponds to a reduction in surface roughness of approximately 17–18% compared to the highest Rt values recorded at the lowest rotational speed used in the experiments. The most favorable feed rate per revolution, for which the Rt parameter value of (Rt =

**Table 3.** ANOVA statistical analysis for the roughness Rt drilled in 40HM+QT

| Source | SS | DF | MS | F | p | PC |
|---|---|---|---|---|---|---|
| Model | 3.6093 | 9 | 0.4010 | 5.9780 | 0.0008 | |
| Constant | 0.2835 | 1 | 0.2835 | 4.2264 | 0.0555 | |
| n | 0.6583 | 1 | 0.6583 | 9.8135 | 0.0061 | 21.84 |
| $n^2$ | 0.4486 | 1 | 0.4486 | 6.6866 | 0.0192 | 14.89 |
| $f_n$ | 0.1893 | 1 | 0.1893 | 2.8221 | 0.1113 | 6.28 |
| $f_n^2$ | 0.1129 | 1 | 0.1129 | 1.6827 | 0.2119 | 3.75 |
| KIN | 0.4155 | 1 | 0.4155 | 6.1936 | 0.0235 | 13.79 |
| KIN2 | 0.3510 | 1 | 0.3510 | 5.2316 | 0.0353 | 11.65 |
| n·fn | 0.2945 | 1 | 0.2945 | 4.3904 | 0.0514 | 9.77 |
| n·KIN | 0.2806 | 1 | 0.2806 | 4.1834 | 0.0566 | 9.31 |
| fn·KIN | 0.2629 | 1 | 0.2629 | 3.9186 | 0.0642 | 8.72 |
| Error | 1.1405 | 17 | 0.0671 | | | 24.01 |
| Total | 4.7498 | 26 | | | | 100.00 |

KIN: Kinematic system.

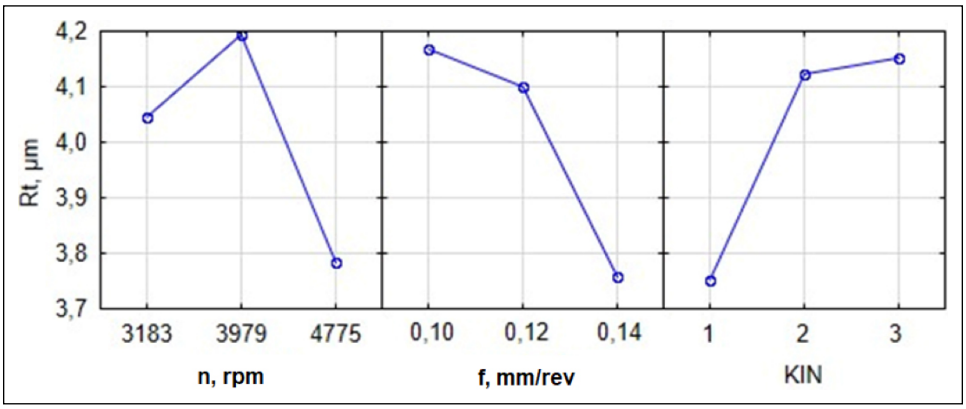


**Figure 10**. The main effects plot for Rt.

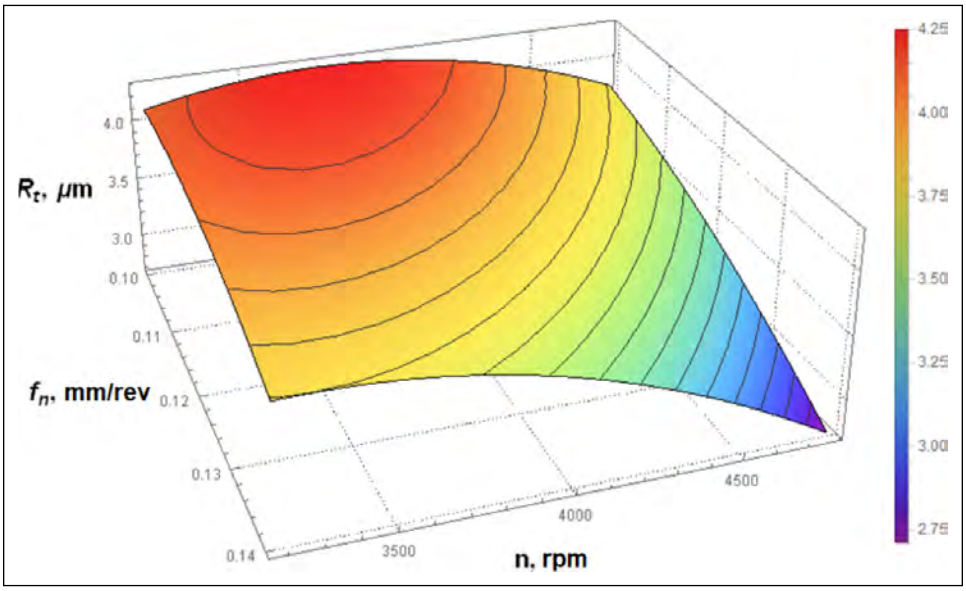


**Figure 11**. Influence of technological parameters in the first kinematics on the Rt parameter of a hole in heat-treated 40HM+QT steel based on equation (3).

3.758 µm) was obtained, is 0.14 mm/rev, representing an improvement in surface roughness of approximately 10-12% in comparison with the least favorable feed rate applied in this study. Using the first kinematic system in the process of drilling heat-treated 40HM+QT steel, the lowest Rt parameter value of 3.751 µm was obtained, which is approximately 18-19% lower than the Rt values obtained using the third kinematic system. It was observed that reducing feed per revolution generally decreases the Rt value.

Graphical simulations based on response surface regression (RSM) enable visual representation of the relationship between input parameters (spindle speed, feed rate per revolution, and kinematic drilling variant) and output responses (surface roughness Rt). The developed models provide a consistent tool for assessing the impact of technological variables on hole quality and allow for comparison of the effectiveness of different drilling process variants.

Analyzing Figure 11 for the first kinematic system, it was found that using the highest tested feed rate per revolution of 0.14 mm/rev and the highest spindle speed of 4775 rpm, the lowest Rt parameter value was obtained. In this case, changing the spindle speed and feed per revolution significantly worsens the Rt parameter.

When analyzing Figure 12 for the second kinematic system, it was found that using the smallest feed per revolution of 0.1 mm/rev and the lowest spindle speed of 3183 rpm resulted in the lowest Rt parameter value. In this case, using the highest feed value 0.14 mm/rev and the highest tested spindle speed value also resulted in the lowest Rt parameter value.

On the other hand, when analyzing Figure 13 for the third kinematic system, it was noticed that using the highest feed rate per revolution of 0.14 mm/rev and the highest spindle speed of 4775 rpm resulted in the lowest Rt parameter.

## CONCLUSION

The experimental results clearly demonstrate that the kinematic system applied during drilling plays a decisive role in shaping the surface roughness of holes machined in heat-treated 40HM+QT steel. Based on the Taguchi L27 design, ANOVA, and RSM modeling, the following conclusions can be drawn:

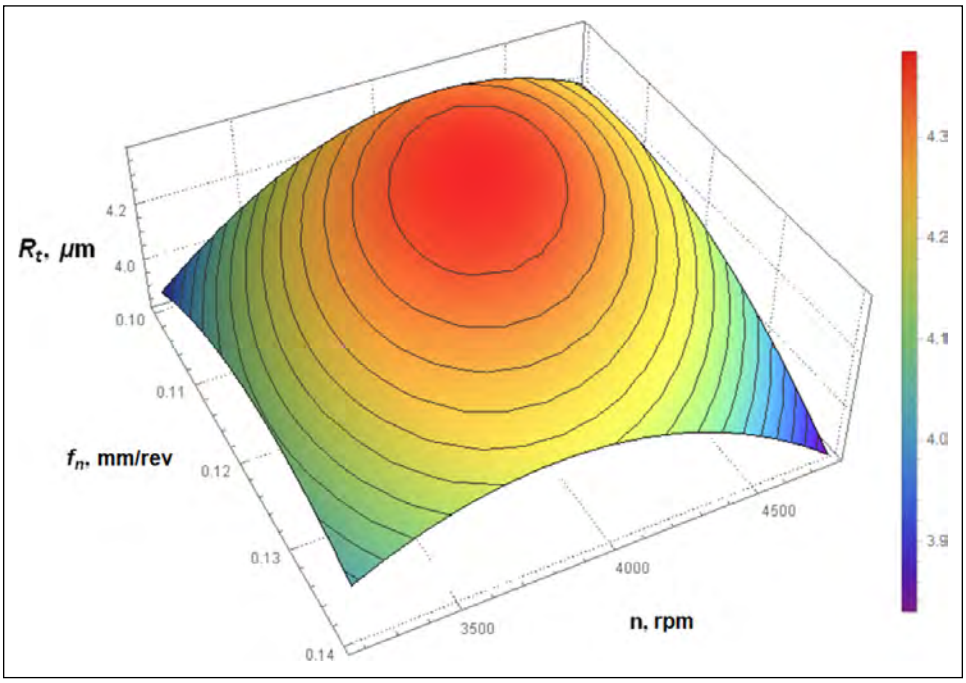


**Figure 12**. Influence of technological parameters in the second kinematics on the Rt parameter of a hole in heat-treated 40HM+QT steel based on equation (3).

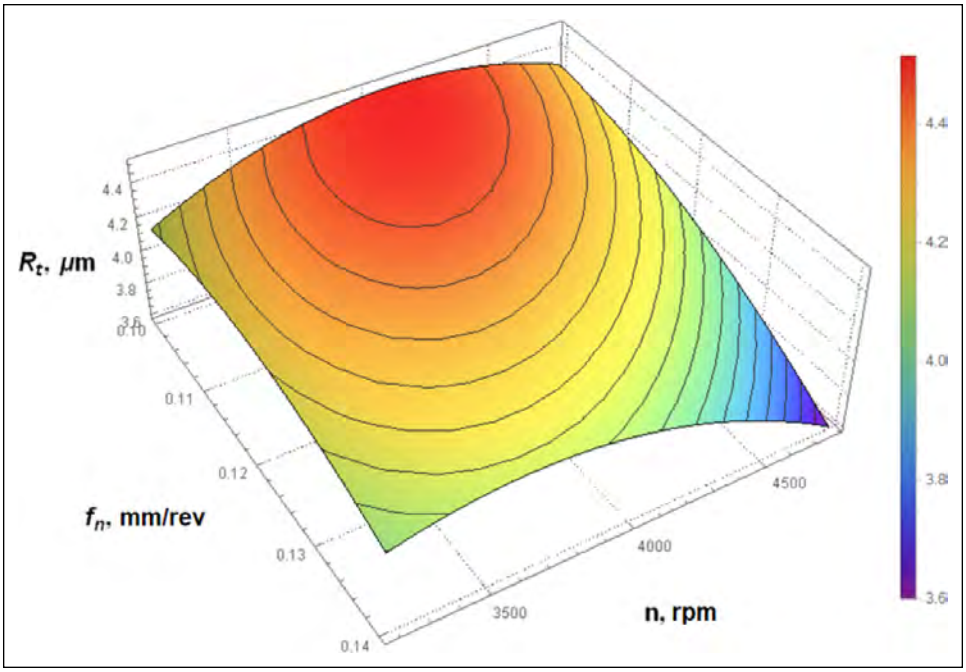


**Figure 13**. Influence of technological parameters in the third kinematics on the Rt parameter of a hole in heat-treated 40HM+QT steel based on equation (3).

- Spindle speed (n) was the dominant factor, accounting for 46.27% of the total influence on the Rt parameter. Higher spindle speeds generally resulted in lower roughness values due to more stable chip formation and reduced cutting force fluctuations.
- The kinematic system contributed 34.45%, confirming that the way rotational and feed motions are distributed between the tool and the workpiece has a substantial impact on the dynamic behavior of the process.
- The first kinematic system, combining tool rotation with an additional axial oscillation, provided the lowest overall Rt values (3.75 μm).
- The oscillatory component improves chip evacuation and reduces built-up edge formation, resulting in smoother surface profiles.
- Feed per revolution (19.28% contribution) showed a less pronounced but still relevant effect.
- Interestingly, the lowest Rt values were often obtained at

the highest tested feed of $f_n$ = 0.14 mm/rev, which suggests more stable chip segmentation within the tested range.
- RSM visualizations confirmed that the combination of high spindle speed and the first kinematic system forms the most favorable drilling conditions for achieving minimal Rt values.
- The results also show that for the second and third kinematic systems, optimal parameter windows differ significantly, indicating that each kinematic variant should be optimized independently rather than by direct parameter translation.
- Overall, the study demonstrates that non-traditional kinematic systems can significantly improve surface roughness in drilling heat-treated steels, and may be considered a practical alternative for boosting hole quality without additional technological modifications.
- The findings provide a foundation for future optimization of drilling operations in difficult-to-cut materials and indicate that kinematic configuration should be treated as a primary process parameter rather than an auxiliary factor.

**Data Availability Statement**

The authors confirm that the data that supports the findings of this study are available within the article. Raw data that support the finding of this study are available from the corresponding author, upon reasonable request.

**Author's Contributions**

Mehmet Şükrü Adin: Conception, Design, Supervision, Analysis and Interpretation, Literature Review, Writer, Critical Review.

Mateusz Bronis: Conception, Materials, Design, Data Processing, Supervision, Analysis and Interpretation, Literature Review, Writer, Critical Review.

**Conflict of Interest**

The authors declared no potential conflicts of interest with respect to the research, authorship, and/or publication of this article.

**Statement on the Use of Artificial Intelligence**

Artificial intelligence was not used in the preparation of the article.

**Ethics**

There are no ethical issues with the publication of this manuscript.

**Funding**

The author declare that no funds, grants, or other support were received during the preparation of this manuscript.

## REFERENCES

[1] Kowalska, N., Błasiak, S., Skrzyniarz, M., Szczygieł, P., Szot, W., & Rudnik, M. (2025). Evaluation of surface roughness reduction in TPU 95A samples using ferromagnetic liquid machining. *Materials, 18*, Article 4939. [CrossRef]

[2] Bronis, M., Miko, E., Nowakowski, L., & Bartoszuk, M. (2022). A study of the kinematics system in drilling Inconel 718 for improving hole quality in the aviation and space industries. *Materials, 15*, Article 5500. [CrossRef]

[3] Bronis, M., Miko, E., & Nowakowski, L. (2021). Influence of the kinematic system on the geometrical and dimensional accuracy of holes in drilling. *Materials, 14*, Article 4568. [CrossRef]

[4] Szot, W., Rudnik, M., Szczygieł, P., & Kowalska, N. (2025). Evaluation of tensile stress relaxation of selective laser sintering of PA2200 material using the Maxwell-Wiechert model. *Acta Mechanica et Automatica, 19*, 292-299. [CrossRef]

[5] Bronis, M., Krawczyk, B., & Legutko, S. (2024). Effect of choice of drilling kinematic system on cylindricity deviation, roundness deviation, diameter error and surface roughness of holes in brass alloy. *Processes, 12*, Article 220. [CrossRef]

[6] Sutopo, Wijanarka, B. S., Wibowo, A. E., Arifin, A., & Wu, Y.-R. (2025). Cutting performance of various CNC drilling cycles at diverse cutting speeds concerning hole dimension error, surface roughness, and cutting time. *International Journal of Machining and Machinability of Materials, 27*, 224-250. [CrossRef]

[7] Nowakowski, L., Rolek, J., Błasiak, S., & Skrzyniarz, M. (2024). The influence of insert mounting errors on the surface roughness of 1.0503 steel in face milling. *Materials, 17*, Article 6144. [CrossRef]

[8] Nowakowski, L., Bartoszuk, M., Skrzyniarz, M., Błasiak, S., & Vasileva, D. (2022). Influence of the milling conditions of aluminium alloy 2017A on the surface roughness. *Materials, 15*, Article 3626. [CrossRef]

[9] Nowakowski, L., Bronis, M., Błasiak, S., & Skrzyniarz, M. (2025). A method for determining the minimum thickness of the cut layer in precision milling. *Materials, 18*, Article 189. [CrossRef]

[10] Özcan, D., Özsoy, N., Turgut, Y. Z., & Özsoy, M. (2025). Effects of tool geometry on cutting performance in CW511L brass drilling. *Materials Testing, 68*(1), 96-111. [CrossRef]

[11] Biswas, S., Saikat, C. S., Sristi, N. A., & Zaman, P. B. (2025). A review of the role of modeling and optimization methods in machining Ni-Cr super-alloys. *Journal of Manufacturing and Materials Processing, 9*, Article 289. [CrossRef]

[12] Bronis, M., Miko, E., & Nowakowski, L. (2021). Analyzing the effects of the kinematic system on the quality of holes drilled in 42CrMo4 + QT steel. *Materials, 14*, Article 4046. [CrossRef]

[13] Balaji, M., Venkata Rao, K., Mohan Rao, N., & Murthy, B. S. N. (2018). Optimization of drilling parameters for drilling of Ti-6Al-4V based on surface roughness, flank wear and drill vibration. *Measurement, 114*, 332-339. [CrossRef]

[14] Kumar, D., & Sing, K. K. (2017). Experimental analysis of delamination, thrust force and surface roughness on drilling of glass fibre reinforced polymer

composites material using different drills. *Materials Today: Proceedings, 4*, 7618-7627. [CrossRef]

[15] Kilickap, E., Huseyinoglu, M., & Yardimeden, A. (2011). Optimization of drilling parameters on surface roughness in drilling of AISI 1045 using response surface methodology and genetic algorithm. *International Journal of Advanced Manufacturing Technology, 52*, 79-88. [CrossRef]

[16] Aized, T., & Amjad, M. (2013). Quality improvement of deep-hole drilling process of AISI D2. *International Journal of Advanced Manufacturing Technology, 69*, 2493-2503. [CrossRef]

[17] Ravindranath, V. M., Shiva Shankar, G. S., Basavarajappa, S., & Suresh, R. (2017). Optimization of Al/B4C and Al/B4C/Gr MMC drilling using Taguchi approach. *Materials Today: Proceedings, 4*, 11181-11187. [CrossRef]

[18] Vipin, Kant, S., & Jawalkar, C. S. (2018). Parametric modeling in drilling of die steels using Taguchi method based response surface analysis. *Materials Today: Proceedings, 5*, 4531-4540. [CrossRef]

[19] Aamir, M., Tolouei-Rad, M., Giasin, K., & Vafadar, A. (2020). Machinability of Al2024, Al6061, and Al5083 alloys using multi-hole simultaneous drilling approach. *Journal of Materials Research and Technology, 9*, 10991-11002. [CrossRef]

[20] Angelone, R., Caggiano, A., Improta, I., Nele, L., & Teti, R. (2020). Roughness of composite materials: Characterization of hole quality in drilling of Al/CFRP stacks. *Procedia CIRP*, 88, 473-478. [CrossRef]

[21] Khanna, N., Agrawal, C., Gupta, M. K., & Song, Q. (2020). Tool wear and hole quality evaluation in cryogenic drilling of Inconel 718 superalloy. *Tribology International, 143*, Article 106084. [CrossRef]

[22] Biermann, D., Heilmann, M., & Kirschner, M. (2011). Analysis of the influence of tool geometry on surface integrity in single-lip deep hole drilling with small diameters. *Procedia Engineering, 19*, 16-21. [CrossRef]

[23] Wegert, R., Guski, V., Schmauder, S., & Möhring, H.-C. (2020). Effects on surface and peripheral zone during single lip deep hole drilling. *Procedia CIRP, 87*, 113-118. [CrossRef]

[24] Siddique, M. Z., Faraz, M. I., Butt, S. I., Khan, R., Petru, J., Jaffery, S. H. I., Khan, M. A., & Tahir, A. M. (2023). Parametric analysis of tool wear, surface roughness and energy consumption during turning of Inconel 718 under dry, wet and MQL conditions. *Machines, 11*, Article 1008. [CrossRef]

[25] Gowda, B. M. U., Ravindra, H. V., Prakash, G. V. N., Nishanth, P., & Ugrasen, G. (2015). Optimization of process parameters in drilling of epoxy Si3N4 composite material. *Materials Today: Proceedings, 2*, 2852-2861. [CrossRef]

[26] Prakash, S., Mercy, J. L., Salugu, M. K., & Vineeth, K. S. M. (2015). Optimization of drilling characteristics using grey relational analysis (GRA) in medium density fiber board (MDF). *Materials Today: Proceedings, 2*, 1541-1551. [CrossRef]

[27] Sharman, A. R. C., Amarasinghe, A., & Ridgway, K. (2008). Tool life and surface integrity aspects when drilling and hole making in Inconel 718. *Journal of Materials Processing Technology, 200*, 424-432. [CrossRef]

[28] Neo, D. W. K., Liu, K., & Kumar, A. S. (2020). High throughput deep-hole drilling of Inconel 718 using PCBN gun drill. *Journal of Manufacturing Processes, 57*, 302-311. [CrossRef]

[29] Karabulut, Y., & Kaynak, Y. (2020). Drilling process and resulting surface properties of Inconel 718 alloy fabricated by selective laser melting additive manufacturing. *Procedia CIRP, 87*, 355-359. [CrossRef]

[30] Shah, P., Bhat, P., & Khanna, N. (2021). Life cycle assessment of drilling Inconel 718 using cryogenic cutting fluids while considering sustainability parameters. *Sustainable Energy Technologies and Assessments, 43*, Article 100950. [CrossRef]

[31] Dedeakayoğulları, H., Kaçal, A., & Keser, K. (2022). Modeling and prediction of surface roughness at the drilling of SLM-Ti6Al4V parts manufactured with pre-hole with optimized ANN and ANFIS. *Measurement, 203*, Article 112029. [CrossRef]

[32] Dedeakayoğulları, H., & Kaçal, A. (2022). Experimental investigation of hole quality in drilling of additive manufacturing Ti6Al4V parts produced by hole features. *Journal of Manufacturing Processes, 79*, 745-758. [CrossRef]

[33] Güldibi, A., Köklü, U., & Koçar, O., Kocaman, E., & Morkavuk, S. (2024). The effects of aging process after solution heat treatment on drilling machinability of Corrax steel. *Experimental Techniques, 48*, 239-257. [CrossRef]

[34] Baysal, E., Koçar, O., & Kahrıman, F., & Köklü, U. (2025). Investigation of microstructure, hardness, corrosion and machinability properties of commercially pure aluminum alloyed with rare-earth elements. *International Journal of Metalcasting*, Preprint. doi: 10.1007/s40962-025-01655-y [CrossRef]

[35] Callister, W. D., & Rethwisch, D. G. (2014). *Materials science and engineering: An introduction* (9th ed.). Wiley.

[36] Nguyen, V. H., Le, T. T., Nguyen, A. T., Hoang, X. T., Nguyen, N. T., & Nguyen, N. K. (2025). Optimization of milling conditions for AISI 4140 steel using an integrated machine learning-multi objective optimization-multi criteria decision making framework. *Measurement, 242*, Article 115837. [CrossRef]

J Adv Manuf Eng, Vol. 7, Issue. 1, pp. 11–20, June, 2026

Journal of Advances in Manufacturing Engineering
Web page info: https://jame.yildiz.edu.tr
DOI: 10.14744/ytu.jame.2026.00002

Original Article

# Investigation of the deformation and thrust forces generated during the drilling of GFRP composites

**Yunus Emre NEHRİ[1], Mert ŞENER[1], Sıla Betül KİRZUK[1], Sudem ÇETİNER[1], Osman Talha DİNÇER[2], Ali ORAL[*,1,3]**

[1]*Department of Mechanical Engineering, Faculty of Engineering, Balikesir University, Balıkesir, Türkiye*
[2]*GENBA Group, Balıkesir, Türkiye*
[3]*ArgeoN Teknoloji Mühendislik Hizmetleri, Balıkesir, Türkiye*

**ARTICLE INFO**

*Article history*
Received: 09 December 2025
Revised: 07 January 2026
Accepted: 13 January 2026

**Key words:**
Delamination, desirability function, drilling, GFRP, hole taper, thrust forces.

**ABSTRACT**

Glass fiber-reinforced polymer (GFRP) composites are widely used in industry due to their advantageous properties, such as a high strength-to-weight ratio. However, during the preparatory processes for bolted or riveted joints, drilling operations often lead to delamination damage, which adversely affects the mechanical performance and reliability of these materials. In this study, the effects of different cutting speeds and feeds on thrust force and delamination damage during the drilling of GFRP composites were investigated. The maximum thrust forces generated during the hole drilling process were measured, and post-drilling deformations were examined. Mathematical models were developed using the response surface method (RSM) to predict thrust force and delamination under various cutting conditions determined by the selected drill geometry. The results of the analysis of variance (ANOVA) showed that the developed models were statistically significant with a confidence level of over 90%. It was found that feed is the dominant parameter influencing thrust force, whereas cutting speed plays a primary role in determining the extent of delamination. The results provide valuable insights for establishing optimum cutting conditions aimed at minimizing drilling damage in GFRP composite machining.

**Cite this article as:** Nehri, Y. E., Şener, M., Kirzuk, S.B., Çetiner, S., Dinçer, O.T., & Oral, A. (2026). Investigation of the deformation and thrust forces generated during the drilling of GFRP composites. *J Adv Manuf Eng*, 7(1), 11–20.

## INTRODUCTION

Glass fibre reinforced polymer (GFRP) composite materials, which are indispensable in engineering applications, are widely used in many industries such as wind turbine manufacturing, automotive, aerospace, and marine due to their lightweight nature and cost-effectiveness [1–3]. Although composite materials are generally manufactured in shapes close to the final geometry, machining operations such as drilling are often required to achieve assembly requirements or dimensional tolerances [3–5]. During the drilling process, problems such as delamination, fibre pull-out, fibre breakage, micro-cracks, and poor hole surface quality are encountered due to the layered and anisotropic structures of composite materials. These problems compromise material integrity, reduce strength, and may lead to parts being scrapped during the production process. Therefore, minimizing damage during drilling, specifically achieving high hole surface quality with minimal delamination and thrust force, is of critical importance. Deter-

***Corresponding author.**
*E-mail address: a.oral@balikesir.edu.tr

mining the optimum hole drilling parameters according to experimental designs by avoiding multiple experiments to determine the minimum damage is important in terms of time efficiency, cost reduction, and improved manufacturing quality [5–10].

Errors that occur after drilling are generally associated with factors such as incorrect drilling parameters, improper selection of the cutting tool, and thrust force. Numerous studies in the literature indicate that feed rate has a significant effect on delamination and thrust force [9,11–15]. These studies generally report that the thrust force and delamination increase with increasing feed or feed rate [5,9,10,16], while no significant increase or decrease is observed with increasing cutting speed [15,17–22]. The temperature increase in the hole region resulting from increasing cutting speed can cause local softening of the composite material, reducing the thrust force, alternatively may increase delamination due to undesirable effects such as fiber entanglement without softening [3]. Increasing the diameter of the cutting tool, one of the parameters affecting delamination and thrust force, increases delamination and thrust force [5]. Since the hole diameter is known during the assembly process, no change in the drill diameter is required. However, the effect of the drill tip geometry on delamination and thrust force is of critical importance. It has been reported that better results are obtained at lower point angles in the drilling of GFRP composite materials [9,23].

Various analysis and optimization methods are used to overcome processing difficulties, such as delamination in drilling operations, and to determine optimal drilling parameters. Abdul Nasir et al. [22] emphasized that feed rate, rather than cutting speed, is the dominant parameter affecting thrust force in the drilling of flax fiber composites. Ertürk et al. [20] investigated the drilling characteristics with different drill geometries, feed rates, and cutting speed parameters, and analyzed their experimental results using the response surface method. They reported that thrust force and cutting torque increased with increasing feed rate, while cutting speed had no significant effect. They also emphasized that the drill tip coating is a significant factor affecting the sample temperature during drilling.

Karimi et al. [24] investigated the effects of the nanomaterial content in the composite structure, drill diameter, feed rate, and cutting speed on drilling conditions. According to ANOVA results, they emphasized that the effect of drill diameter on delamination is negligible, while feed rate has the most significant effect. They concluded that there was a significant interaction between the feed rate and the cutting speed. Karaca [25] investigated the effects of cutting speed, feed rate, and drill tip angle on exit delamination and emphasised that cutting speed has no significant effect, while feed rate and drill tip angle strongly influence the delamination factor. Also, the study reported that low feed rates combined with small tip angles yield minimal deformation. Shanmugam et al. [26] investigated the effects of drill bit angle, feed rate, and cutting speed on thrust force, delamination, and burr formation. They reported that thrust force increases with higher feed rates and cutting speeds and that a 118° drill tip angle results in lower thrust forces. ANOVA results showed that thrust force is influenced primarily by cutting speed, followed by feed rate and drill tip angle, while delamination is significantly affected by feed rate. Kalita et al. [14] examined the effects of material thickness, drill diameter, cutting speed, and feed rate, each at three levels, on delamination. They concluded that delamination decreases with increasing material thickness and decreasing feed rate. While feed rate had a dominant effect on delamination, cutting speed had no significant effect. To determine the minimum delamination factor, they employed Genetic Algorithm (GA) and Particle Swarm Optimization (PSO), emphasising that both methods converged to the same optimal solution, although PSO achieved faster performance. Behera et al. [27] investigated the entry delamination factor and surface roughness values (Ra-Rq) using the parameters of material thickness, drill diameter, cutting speed, and feed rate during the drilling process. Using artificial neural networks (ANN), they established predictive relationships and analyzed the results. Experimental findings indicated that feed rate is the most influential parameter for both output responses. They concluded that delamination decreased with increasing material thickness and decreasing feed rate, while surface roughness increased with higher feed rate. Spindle speed was found to have no significant effect. Xu et al. [21] investigated drilling experiments using different feed rates, cutting speeds, and drill bits (double-edged and dagger-drills). Xu et al. [21] conducted drilling experiments using different feed rates, cutting speeds, and drill bits (double-edged and dagger-drills). They examined the effects of the parameters on cutting forces, machining temperatures, and delamination as a result of the drilling process. They noted that cutting speed had no significant effect on thrust force, but plays a major role in temperature generation. They also demonstrated that drilling could be performed without delamination using a double-point-angle drill. Biruk-Urban et al. [28] investigated the effects of cutting speed and feed rate on drilling four different types of GFRP composites, each with varying fiber weight fractions and fiber type (Twill and Plain). They emphasized that Fz, a cutting force component, is significantly affected by the feed rate, and that Fz increases with increasing feed rate. They recommended the use of Twill-type fibers. Abd-Elwahed [4] investigated torque and delamination by machining woven glass fiber-reinforced epoxy composites at different laminate thicknesses, feed rates, and cutting speeds. The results were modeled and evaluated using the response surface methodology (RSM) and artificial neural networks (ANN). By enhancing ANN training with particle swarm optimization (PSO), the prediction performance of the models was improved. The study highlighted that low feed rates and high cutting speeds lead to optimal values for torque and delamination.

Generally, low cutting speeds and feeds/feed rates are recommended to minimize delamination. Although previous research has addressed various drilling problems with GFRP composites, a comprehensive understanding of drilling behavior and damage mechanisms has not yet been fully established in the industry.

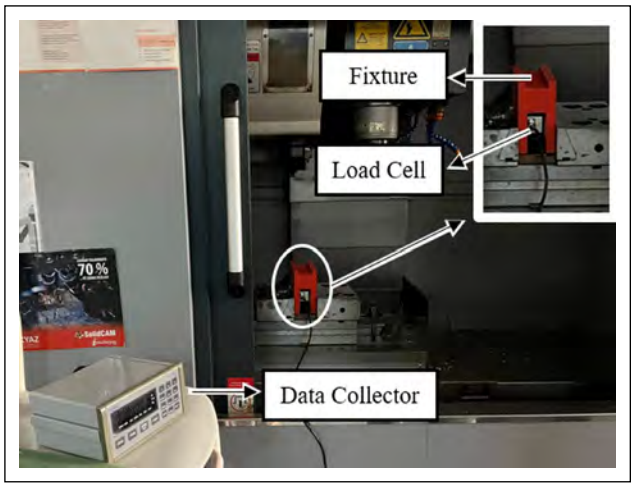


**Figure 1**. Experimental system.

**Figure 2**. SDC drill bit.

**Table 1.** Cutting parameters and levels

| Parameters | Levels |
|---|---|
| Cutting Speed – $V_c$ (m/min) | 80 – 100 – 120 |
| Feed – f (mm/rev) | 0.05 – 0.0625 – 0.075 – 0.0875 – 0.1 |

In this study, the effects of cutting speed and feed on delamination and cutting forces (thrust force) were investigated during drilling 10 mm diameter holes using an SDC drill bit in the drilling process of GFRP composite materials. Drilling experiments were conducted at five different feeds and three different cutting speeds. As output responses, delamination, hole taper, and thrust force were evaluated. Analysis of variance was performed, and mathematical models were developed using the response surface method. By examining the effects of input parameters on output values, optimum cutting parameters for improved hole quality in GFRP drilling were determined using RSM combined with the desirability function approach. Comparsion with experimental results confirmed the strong predictive capability of the developed models.

## MATERIALS AND METHODS

In this study, drilling operations using a special SDC series drill bit were performed on glass fiber–reinforced polymer (GFRP) composite materials that were commercially manufactured using the vacuum infusion method. The GFRP composites were produced by GENBA using a 16-ply vacuum infusion method using 0/90° plain woven fabrics. The manufactured composites were cut into specimens with dimensions of 8.6 × 35 × 200 mm using a water-jet cutting to prepare them for experimentation. Drilling experiments operations were conducted on a LER VQ-75 CNC vertical machining center with a spindle motor power of 20 kW and a spindle speed range of 50-11000 rpm (Fig. 1). An MDS10000SDC3-coded drill bit with a diameter of Ø10 mm (Fig. 2) was used in the experiments, which were conducted under air cooling conditions. The study was conducted using a Multilevel Factorial experimental design with three different cutting speeds and five different feeds as cutting parameters, and a total of 15 experiments were conducted (Table 1). The flowchart of the experimental study is presented in Figure 3.

To ensure accurate measurement of the thrust force during drilling, a protective fixture was designed to isolate the load cell from external factors (Fig. 4). The thrust forces generated during the drilling process (Fig. 5), performed at different levels and parameters, were measured using an MS Cell SS300 series load cell with a capacity of 500 kg. Delamination occurring on the upper surface of the specimens after drilling was examined using a Dino-Lite Pro AM4000 series digital microscope equipped with a 1.3-megapixel camera.

As a result of the experiments, variance analysis was applied to investigate the effects of input parameters on delamination, hole taper (conicity), and thrust force. The aim was to determine the cutting speed and feed values that minimize delamination, hole taper, and thrust force. Due to the limited number of experimental data points, optimization was performed using the RSM combined with the Desirability Function approach, which is suitable for small datasets [29].

## RESULTS AND DISCUSSION

Drilling GFRP composites, widely used in industry, is difficult due to delamination. Regions affected by delamination a reduction in material strength [1], which can lead to assembly errors, non-compliance with tolerance requirements, and ultimately the rejection of manufactured parts or failure to meet the design specifications. These problems were controlled by optimizing cutting parameters to achieve minimum delamination and thrust force.

The results of the thrust force, delamination factor, and hole taper, resulting from feed and cutting speeds, are shown in Figure 6. It was observed that decreasing the feed resulted in a reduction in thrust force, delamination factor, and hole taper. The delamination factor and hole taper also decreased with decreasing cutting speed. While the thrust force was low at the upper and lower cutting speed values, the thrust force was high at the middle cutting speed values. Variance analysis was preferred to examine the relationship between the input parameters and the output responses.

Analysis of Variance (ANOVA) is a statistical analysis technique used to determine the significance of independent variables, called input parameters, on the output responses obtained because of the input parameters. ANOVA

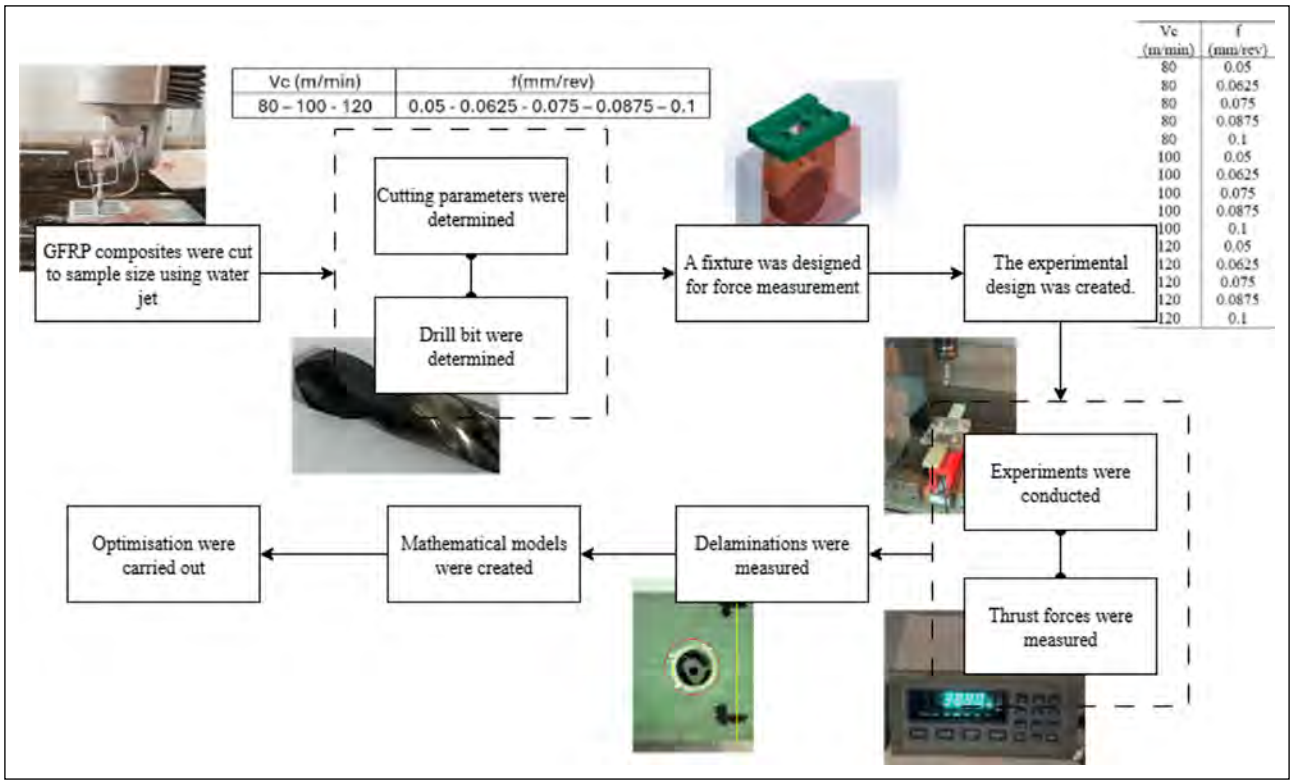


**Figure 3**. Flowchart.

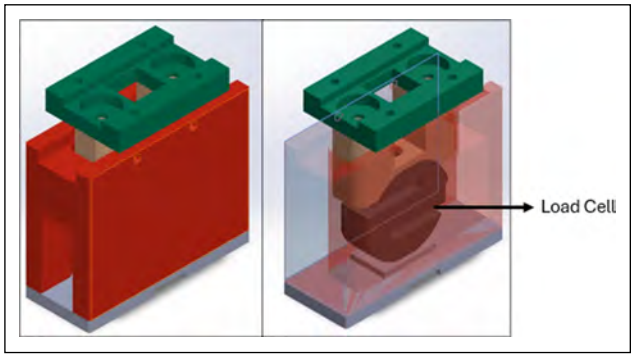


**Figure 4**. Load cell protective fixture.

determines the effect ratios of input parameters on output responses. It also determines whether there is a significant relationship between input parameters and output responses [30]. Variance analysis at a 95% confidence level for thrust force, delamination factor, and hole taper is presented in Table 2. The table includes the percentage contributions and p-values for individual parameters and their interactions. P-values lower than 0.05 indicate that the corresponding parameter has a statistically significant effect on the output response.

Examination of the ANOVA results indicated that both cutting speed and feed have a significant effect on thrust force, delamination, and hole taper. Feed was the most effective parameter on thrust force, whereas cutting speed had a greater effect on delamination and hole taper. Mahesh et al. [31] also reported in their study that cutting speed was the most effective parameter on delamination and that cutting speed had a greater impact on taper than feed.

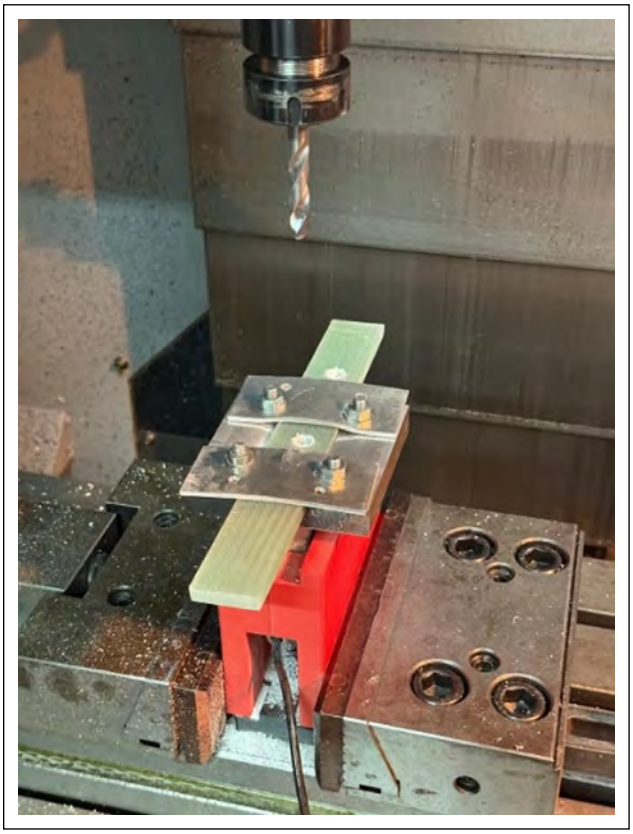

**Figure 5**. Test sample.

The response surface method is an empirical modeling approach used to determine the relationship between different input parameters and output responses [30, 32].

**Table 2.** ANOVA results for thrust force, delamination factor, and hole taper

| Output | Fz | | Df | | C | |
|---|---|---|---|---|---|---|
| **Source** | **Contribution** | **P-Value** | **Contribution** | **P-Value** | **Contribution** | **P-Value** |
| Model | 98.77% | 0.000 | 94.89% | 0.000 | 91.87% | 0.000 |
| Linear | 70.23% | 0.000 | 50.13% | 0.000 | 39.88% | 0.000 |
| $V_c$ (m/min) | 5.42% | 0.000 | 33.61% | 0.000 | 28.66% | 0.000 |
| f (mm/rev) | 64.81% | 0.000 | 16.52% | 0.000 | 11.22% | 0.006 |
| Square | 23.38% | 0.000 | 13.33% | 0.003 | 25.81% | 0.002 |
| $V_c$ (m/min)*$V_c$ (m/min) | 22.96% | 0.000 | 13.30% | 0.001 | 25.72% | 0.000 |
| f (mm/rev)*f (mm/rev) | 0.43% | 0.110 | 0.04% | 0.807 | 0.09% | 0.754 |
| 2-Way Interaction | 5.16% | 0.000 | 31.42% | 0.000 | 26.18% | 0.000 |
| $V_c$ (m/min)*f (mm/rev) | 5.16% | 0.000 | 31.42% | 0.000 | 26.18% | 0.000 |
| Error | 1.23% | | 5.11% | | 8.13% | |
| Total | 100.00% | | 100.00% | | 100.00% | |

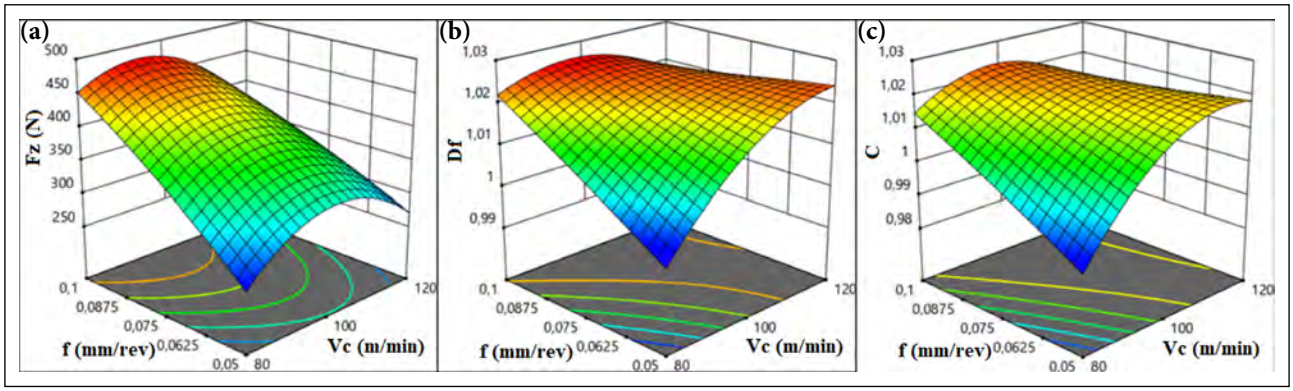


**Figure 6**. Flowchart.

In order to determine the effects of feed and cutting speed factors, second-order mathematical models were developed using the response surface methodology for the outputs of thrust force, delamination, and hole taper. Based on the experimental data, Equation 1, Equation 2, and Equation 3 represent the relationship function between the input parameters and the measured outputs. Where ε represents unexplained experimental errors.

Output function for the thrust force:

$$Fz=f(Vc,f)+\varepsilon \quad (1)$$

Output function for the delamination factor:

$$Df=f(Vc,f)+\varepsilon \quad (2)$$

Output function for the hole taper:

$$C=f(Vc,f)+\varepsilon \quad (3)$$

The second-order equations based on the Response Surface Method are given in Equation 4, Equation 5, and Equation 6.

$$Fz=\beta_0+\beta_1.V_c+\beta_2.f+\beta_3.V_c.V_c+\beta_4.f.f+\beta_5.f.V_c \quad (4)$$

$$Df=\beta_0+\beta_1.V_c+\beta_2.f+\beta_3.V_c.V_c+\beta_4.f.f+\beta_5.f.V_c \quad (5)$$

$$C=_0+\beta_1.V_c+\beta_2.f+\beta_3.V_c.V_c+\beta_4.f.f+\beta_5.f.V_c \quad (6)$$

The regression equations with a confidence interval of 95% have a confidence level of 98.77%, 94.89%, and 91.87%, respectively. The regression equations generated using the Response Surface Method are given in Equation 7, Equation 8, and Equation 9.

$$Fz=-1787+35.01*V_c+10241*f-0.1609*V_c^2-15829*f^2-49.83*f*V_c \quad (7)$$

$$Df=0.6979+0.004646*V_c+1.866*f-0.000016*V_c^2-0.59*f^2-0.01589*f*V_c \quad (8)$$

$$C=0.5567+0.00714*V_c+2.171*f-0.000027*V_c^2-1.19*f^2-0.018*f*V_c \quad (9)$$

When the relationships between the input parameters (independent variable) and the output values (dependent variable) were examined, the coefficient of determination ($R^2$) for the explanatory power of the models was found to be 98.95% for thrust force, 95.75% for delamination factor, and 93.9% for hole taper. The predictive capability of the models was determined as 96.52% for thrust force, 87.96% for delamination factor, and 74.97% for hole taper (Table 3).

**Table 3.** Explanatory power of models

| Output Respose | $R^2$ (%) | $R^2$ adj (%) | $R^2$ pred (%) |
|---|---|---|---|
| Thrust Force - Fz (N) | 98.95 | 98.37 | 96.52 |
| Delamination factor - Df | 95.75 | 93.39 | 87.96 |
| Hole taper (conicity) - C | 93.9 | 90.52 | 74.97 |

**Table 4.** The objective/target and importance levels of optimization

| Output / response | Objective | Target value | Upper limit value | Degree of importance |
|---|---|---|---|---|
| Fz | Minimize | 262.908 | 478.728 | 2 |
| Df | Minimize | 1 | 1.026 | 5 |
| C | Minimize | 1 | 1.027 | 4 |

**Table 5.** Combined desirability optimization outputs

| Combined desirability | Vc (m/min) | f (mm/rev) | Fz (N) | Df | C |
|---|---|---|---|---|---|
| 1 | 80 | 0.05 | 257.504 | 0.997≅1 | 0.987≅1 |

A statistically significant relationship was observed between the input parameters and the output responses.

The high-reliability mathematical models developed in this study enable the prediction of thrust force and the resulting deformation during drilling within the defined drill bit and parameter ranges, without conducting experiments.

Increasing the feed rate from 0.05 mm/rev to 0.1 mm/rev led to a substantial rise in thrust force from 262 N to 478 N. This trend agrees well with results commonly reported in the literature; however, the absolute force levels are higher than those in some studies due to differences in specimen thickness and drill diameter. For example, Vankanti and Ganta reported a maximum thrust force of approximately 78 N when drilling 4 mm thick GFRP laminates using a 10 mm HSS drill [33], whereas the minimum thrust force measured in the present study was 262 N, primarily due to the more than twofold increase in laminate thickness (8.6 mm). Similarly, Abrão et al. [5] reported thrust force values of around 140 N for 2.5 mm thick GFRP laminates drilled with 5 mm diameter tools. In contrast, Latha et al. [34] observed thrust forces of up to 270 N using different drill geometries, which closely match the lower thrust force levels obtained in this study.

The delamination factor values obtained in the present study range from 0.999 to 1.026, indicating markedly superior hole quality compared to previously reported results. For instance, Rubio et al. [35] reported delamination factors between 1.151 and 2.143, while Kilickap [17] and Babu et al. [36] documented minimum values of 1.11 and 1.06, respectively. Importantly, even the maximum delamination factor in this study (1.026) remains below these reported minimum values, demonstrating the effectiveness of the SDC-type drill geometry in suppressing delamination. These results are comparable to the low delamination factor of 1.006 reported by Mohan et al. [37] under optimized conditions and indicate a stable drilling performance under the selected parameter ranges.

The Desirability Function approach is a multi-objective optimization technique commonly used for industrial problems with limited data sets. The purpose of multiple response optimization is to determine the conditions that yield the optimal values of the output (response) variables with respect to the indipendent variables. In this method, individual desirability functions are defined for each response. Three different performance outputs were evaluated within the scope of the study: thrust force, delamination factor, and hole taper. Because minimizing output values is crucial, optimization was performed using the " smaller is better" approach for all criteria.

The desirability value (di) for each output value was normalized between 0 and 1. The desirability value can assume values of 0, between 0 and 1, or 1. If the response value is less than the minimum value, the desirability value is di=1. If the response value is greater than the maximum value, the desirability value is di=0. If the response value is between the minimum and maximum values, the desirability value is between 0 and 1. The overall or combined desirability (D) evaluates how input parameters optimize a set of responses. Combined desirability is the weighted geometric mean of the individual desirability for the results, that is, the responses (Equation 10).

$$D = (d_1^{w1} * d_2^{w2} * \ldots * d_n^{wn})^{1/w} \quad (10)$$

Here, n represents the number of response values, w represents the sum of the individual weights, where the sum of the weights equals one. The weight determines how the desirability is distributed between the lower or upper limits and the target value.

In this study, the three output variables were evaluated simultaneously, and a single optimization model based on the combined desirability function was employed to determine the optimal levels of the input parameters. The targets and objectives were selected separately for each output to accurately determine the effects on the combined desirability. The objective was to minimize the output parameter value. The target values were selected as the minimum of the output values. The weight value can vary between 0.1 and 10 to determine the importance of reaching the target value [38, 39]. During the optimization, the importance levels of the delamination factor and hole taper were set higher than the importance levels of the thrust force. The importance of the parameters was kept high because delamination causes a decrease in the strength of the material, and hole taper causes inconsistency in tolerance values. The objective during optimization was to minimize all output values, and the target was to have no delamination and taper, i.e., that the delamination and taper outputs be equal to one (Table 4).

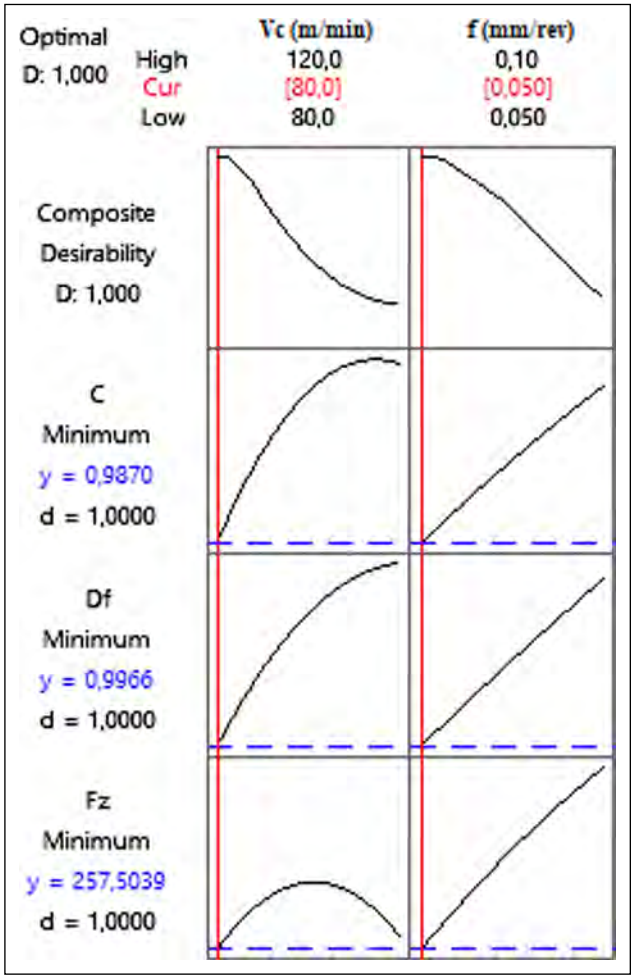


**Figure 7**. Influence plots for optimization of GFRP composite drilling using desirability function.

As a result of the optimization carried out using the defined objectives, targets, and importance weights, the combined desirability value was obtained as 1. A combined desirability value equal to or close to 1 indicates that all optimization criteria were achieved at the target values or at levels better than the targets [30, 40]. This demonstrates that the selected parameter combination represents an optimal point for multi-response optimization. It was observed that minimum cutting speed and feed values provide minimum thrust force, delamination factor, and hole taper. Gemi et al. [7] Abdul Nasir et al. [22] and also reported that the thrust force was lower with decreasing feed, while Kilickap et al. [17] emphasized that lower delamination occurred with low feed and cutting speed, and Shyha et al. [41] emphasized that decreasing feed decreased damage at the entry and exit. The optimum result was obtained at a cutting speed of 80 m/min and a feed value of 0.05 mm/rev. The thrust force was 257.504 N, and the delamination factor and hole taper values were ≅1 (Table 5).

Figure 7 shows the effects of the drilling parameters on individual output values and a set of output values (combined desirability) in the drilling process of a glass fiber-reinforced polymer composite using a desirability function. A linear relationship is observed between feed and the output values, indicating that an increase in feed results in higher values of thrust force, delamination factor, and hole taper. An increase in cutting speed led to a linear increase in hole taper and delamination factor, whereas the thrust force observed a parabolic trend. In the studies by Abd-Elwahed [4] and Birik-Urban et al. [16] a linear increase in thrust force was observed with increasing feed rate, while cutting speed showed lower thrust force values at all levels except at the mid-range level. Similarly, Işık et al. [15] reported a linear relationship between feed rate and cutting force, with lower cutting force observed at the non-linear mid-range level cutting speed. The relatively low influence of cutting speed on thrust force may be attributed to differences in drill geometry and the selected parameter levels, which can result in a non-linear effect. Within the range of the determined parameter levels, it is observed that if the cutting speed is too high or too low, a lower thrust force will be produced. The optimum thrust force occurred at the lowest cutting speed. The three-dimensional graphs of the experimental results clearly match the effect graphs for optimization (Fig. 6, 7).

Gemi et al. [7] and Xu et al. [10] highlighted the importance of drill type in their studies. The drill bits affect delamination at both the entry and exit of the hole. The SDC-type cutting inserts used in this study contribute to the reduction of delamination by reducing the thrust force due to their three-point angles. In addition, the short cutting-edge length, suitable helix angle, and optimized flute geometry of the SDC-type drills limited heat generation, resulting in longer tool life and a stable drilling process [42]. No fiber pull-out or splintering issues were observed during drilling.

Although the present study provides meaningful insights into the optimization of drilling parameters for GFRP composites using RSM and desirability function analysis, certain limitations should be acknowledged. The experimental investigation was restricted to a special drill geometry and a specific GFRP laminate configuration. As a result, the potential effects of different drill point angles, tool coatings, and laminate stacking sequences on thrust force, delamination behavior, and hole quality were not investigated. Therefore, the generalization of the obtained results to other tool designs or composite configurations should be approached with caution. Future studies may extend the current framework by conducting comparative drilling experiments using various drill geometries, such as brad-point, step, or coated drills, as well as GFRP laminates with different fiber orientations and stacking sequences. Moreover, a comparative assessment of holes produced with the same nominal diameter using alternative machining techniques, including abrasive water jet cutting, could provide valuable insights into the differences in damage mechanisms, delamination characteristics, and overall hole quality. Such comprehensive investigations would contribute to a deeper understanding of machining-induced damage in composite materials and enhance the broader applicability of the findings reported in this study.

## CONCLUSIONS

In this study, the drilling of glass fiber-reinforced polymer composite materials using air-cooled special drill bits at different cutting speeds and feed parameters was experimentally investigated. The thrust force generated during the drilling process and the resulting hole deformation damage were examined, and the optimum cutting parameters were determined.

The cutting parameters have a significant effect on thrust force, delamination factor, and hole taper. While the effect of cutting speed on the thrust force is relatively low, the effect of feed is considerably high. The thrust force increases with increasing feed. At a cutting speed of 80 m/min, a 50% increase in feed led to a 35.8% increase in thrust force. At 100 m/min, the same feed increase resulted in a 20.1% rise, and at 120 m/min, a 29.1% increase in thrust force was observed. Conversely, at a feed of 0.05 mm/rev, increasing cutting speed from 80 to 120 m/min (a 25% increase) resulted in a 26.1% rise in thrust force. For feeds of 0.0675, 0.075, 0.0875, and 0.1 mm/rev, the corresponding increases were 19.6%, 11.5%, 7%, and 7%, respectively. Increasing cutting speed from 80 to 120 m/min (50% increase) did not significantly affect thrust force at lower feeds, while at higher feeds, a reduction of approximately 18% was observed. Within the specified parameter range, thrust force was observed to be low at both the lowest and highest cutting speed values. However, the minimum thrust force was obtained at the lowest cutting speed values.

Cutting speed has a greater effect on the delamination factor than feed. Analysis results indicate that the effects of cutting speed and the interaction of cutting speed and feed on the delamination factor are quite high and similar. This also demonstrates the interrelationship of cutting parameters. Minimum delamination was achieved at low cutting speed and feeds.

The effect of cutting parameters on hole taper is similar to that observed for the delamination factor. Cutting speed has a greater effect than feed, and the effects of cutting speed and the interaction of cutting speed and feed on the delamination factor are quite high and similar. Minimum hole taper difference was obtained at low cutting speed and feeds.

The developed models at a 95% confidence interval exhibited reliability levels of 98.95% for thrust force, 95.75% for delamination factor, and 93.9% for hole taper, indicating strong statistical significance. The models are found to be highly significant. The predictive capability of the models was 96.52% for thrust force, 87.96% for delamination factor, and 74.97% for hole taper. These results confirm the high predictive performance of the developed models for the selected parameter ranges.

Optimization using the defined objectives, targets, and importance weights resulted in a combined desirability value of 1. A combined desirability value equal to or close to 1 indicates that all optimization criteria were achieved at or better than the specified target values. As a result of the optimization using the desirability function, the optimum result was achieved at the lowest cutting speed of 80 m/min and the lowest feed of 0.05 mm/rev within the level ranges.

**Acknowledgements**

The authors would like to express their sincere gratitude to Mehmet Gürzoğlu and Sumitomo for their valuable support in supplying the cutting tools used in this study.

**Data Availability Statement**

The authors confirm that the data that supports the findings of this study are available within the article. Raw data that support the finding of this study are available from the corresponding author, upon reasonable request.

**Author's Contributions**

Yunus Emre Nehri: Investigation, Experimental Design, Optimization, Validation, Writing.

Mert Şener: Optimization, Validation, Writing, Original Draft Preparation.

Sıla Betül Kirzuk: Investigation, Experimentation, Design.

Sudem Çetiner: Investigation, Experimentation, Design.

Osman Talha Dinçer: GFRP Manufacturing, Material Supply.

Ali Oral: Methodology, Review, Editing.

**Conflict of Interest**

The authors declared no potential conflicts of interest with respect to the research, authorship, and/or publication of this article.

**Ethics**

The study presented in this paper does not have any ethical issues or no ethical approval was needed to conduct the investigation. The study is not patented or a trade secret of GENBA Group (Balıkesir, Turkey), where Mr. Osman Talha Dinçer is employed.

**Statement on the Use of Artificial Intelligence**

Artificial intelligence was not used in the preparation of the article.

## REFERENCES

[1] Anaç, N., Şen, E., Gül, E., Acar, E., Yıldız, M. E., Koçar, O., & Parmaksız, F. (2025). Investigation of delamination of glass fıber reinforced plastic materials. *Journal of Engineering Sciences and Design, 13*(1), 234-249. [Turkish] [CrossRef]

[2] Koyunbakan, M., Ünüvar, A., Eskizeybek, V., & Avcı, A. (2021). Experimental investigation of CETP composites with wooden drilling performance. *Niğde Ömer Halisdemir University Journal of Engineering Sciences, 10*(2), 770-776. [Turkish] [CrossRef]

[3] Khashaba, U. A. (2023). Mechanics of chip, delamination, and burr formation in drilling supported woven GFRP composites. *Alexandria Engineering Journal, 79*, 181-195. [CrossRef]

[4] Abd-Elwahed, M. S. (2022). Drilling process of GFRP composites: Modeling and optimization using hybrid ANN. *Sustainability, 14*(11), 6599. [CrossRef]

[5] Abrão, A. M., Rubio, J. C. C., Faria, P. E., & Davim, J. P. (2008). The effect of cutting tool geometry on

thrust force and delamination when drilling glass fibre reinforced plastic composite. *Materials & Design, 29*(2), 508-513. [CrossRef]

[6] Kilickap, E. (2011). Analysis and modeling of delamination factor in drilling glass fiber reinforced plastic using response surface methodology. *Journal of Composite Materials, 45*(6), 727-736. [CrossRef]

[7] Gemi, L., Morkavuk, S., Köklü, U., & Gemi, D. S. (2019). An experimental study on the effects of various drill types on drilling performance of GFRP composite pipes and damage formation. *Composites Part B: Engineering, 172*, 186-194. [CrossRef]

[8] Siva Prasad, K., & Chaitanya, G. (2019). Analysis of delamination in drilling of GFRP composites using Taguchi technique. *Materials Today: Proceedings, 18*, 3252-3261. [CrossRef]

[9] Geier, N., & Szalay, T. (2017). Optimisation of process parameters for the orbital and conventional drilling of uni-directional carbon fibre-reinforced polymers (UD-CFRP). *Measurement, 110*, 319-334. [CrossRef]

[10] Xu, J., Li, C., Mi, S., An, Q., & Chen, M. (2018). Study of drilling-induced defects for CFRP composites using new criteria. *Composite Structures, 201*, 1076-1087. [CrossRef]

[11] Ünüvar, A., & Öztürk, O. (2023). Machinability analysis of delamination and thrust force in drilling of pure and added GFRP composites. *Journal of Composite Materials, 57*(1), 3-21. [CrossRef]

[12] Kalidas, V. K., T. G., L., Abu Hassan, S. B., & Chadalavala, H. (2022). A comparative study on drill tool effect on vibration and delamination characteristics of FRPs. *Journal of Natural Fibers, 19*(16), 13943-13957. [CrossRef]

[13] Kavad, B. V., Pandey, A. B., Tadavi, M. V., & Jakharia, H. C. (2014). A review paper on effects of drilling on glass fiber reinforced plastic. *Procedia Technology, 14*, 457-464. [CrossRef]

[14] Kalita, K., Mallick, P. K., Bhoi, A. K., & Ghadai, K. R. (2018). Optimizing drilling induced delamination in GFRP composites using genetic algorithm and particle swarm optimisation. *Advanced Composites Letters, 27*(1), 1-9. [CrossRef]

[15] Işık, I., Batı, S., Demir, M. E., Fidan, S., & Çelik, Y. H. (2025). Symbolic regression analysis of cutting force and delamination in drilling and punching of GFRP composites. *Journal of Reinforced Plastics and Composites*, Preprint. doi:10.1177/07316844251334171 [CrossRef]

[16] Biruk-Urban, K., Bere, P., Józwik, J., & Leleń, M. (2022). Experimental study and artificial neural network simulation of cutting forces and delamination analysis in GFRP drilling. *Materials, 15*(23), 8597. [CrossRef]

[17] Kilickap, E. (2010). Optimization of cutting parameters on delamination based on Taguchi method during drilling of GFRP composite. *Expert Systems with Applications, 37*(8), 6116-6122. [CrossRef]

[18] Kaybal, H. B., Ünüvar, A., Koyunbakan, M., & Avcı, A. (2019). A novelty optimization approach for drilling of CFRP nanocomposite laminates. *The International Journal of Advanced Manufacturing Technology, 100*(9-12), 2995-3012. [CrossRef]

[19] Feito, N., Milani, A. S., & Muñoz-Sánchez, A. (2016). Drilling optimization of woven CFRP laminates under different tool wear conditions: A multi-objective design of experiments approach. *Structural and Multidisciplinary Optimization, 53*(2), 239-251. [CrossRef]

[20] Ertürk, A. T., Vatansever, F., Yarar, E., Güven, E. A., & Sınmazçelik, T. (2021). Effects of cutting temperature and process optimization in drilling of GFRP composites. *Journal of Composite Materials, 55*(2), 235-249. [CrossRef]

[21] Xu, J., Li, L., Geier, N., Davim, J. P., & Chen, M. (2022). Experimental study of drilling behaviors and damage issues for woven GFRP composites using special drills. *Journal of Materials Research and Technology, 21*, 1256-1273. [CrossRef]

[22] Abdul Nasir, A. A., Azmi, A. I., Lih, T. C., & Abdul Majid, M. S. (2019). Critical thrust force and critical feed rate in drilling flax fibre composites: A comparative study of various thrust force models. *Composites Part B: Engineering, 165*, 222-232. [CrossRef]

[23] Gaitonde, V. N., Karnik, S. R., Rubio, J. C., Correia, A. E., Abrão, A. M., & Davim, J. P. (2011). A study aimed at minimizing delamination during drilling of CFRP composites. *Journal of Composite Materials, 45*(22), 2359-2368. [CrossRef]

[24] Karimi, Z., Heidary, H., Yousefi, J., Sadeghi, S., & Minak, G. (2018). Experimental investigation on delamination in nanocomposite drilling. *FME Transactions, 46*(1), 62-69. [CrossRef]

[25] Karaca, F. (2016). Cam elyaf takviyeli plastik kompozitlerde delme parametrelerinin deformasyon faktörüne etkisinin araştırılması. *Science and Engineering Journal of Fırat University, 28*(2), 23-27.

[26] Shanmugam, V., Marimuthu, U., Rajendran, S., Veerasimman, A., Basha, A., Majid, M., Esmaeely Neisiany, R., Försth, M., Sas, G., Razavi, N., & Das, O. (2021). Experimental investigation of thrust force, delamination and surface roughness in drilling hybrid structural composites. *Materials, 14*(16), 4468. [CrossRef]

[27] Behera, R. R., Ghadai, R. K., Kalita, K., & Banerjee, S. (2016). Simultaneous prediction of delamination and surface roughness in drilling GFRP composite using ANN. *International Journal of Plastics Technology, 20*(2), 424-450. [CrossRef]

[28] Biruk-Urban, K., Józwik, J., & Bere, P. (2022). Influence of technological parameters on cutting force components during drilling of GFRP composite. *Proceedings of the IEEE International Workshop on Metrology for AeroSpace*, 81-86. [CrossRef]

[29] Jenarthanan, M. P., & Jeyapaul, R. (2018). Optimisation of machining parameters on milling of GFRP

composites by desirability function analysis using Taguchi method. *International Journal of Engineering, Science and Technology, 5*(4), 22-36. [CrossRef]

[30] Chabbi, A., Yallese, M. A., Meddour, I., Nouioua, M., Mabrouki, T., & Girardin, F. (2017). Predictive modeling and multi-response optimization of technological parameters in turning of polyoxymethylene polymer (POM-C) using RSM and desirability function. *Measurement, 95*, 99-115. [CrossRef]

[31] Mahesh, G. G., & Kandasamy, J. (2023). Experimental investigations on the drilling parameters to minimize delamination and taperness of hybrid GFRP/$Al_2O_3$ composites by using ANOVA approach. *World Journal of Engineering, 20*(2), 376-386. [CrossRef]

[32] Nehri, Y. E., Oral, A., & Toktaş, A. (2025). Optimisation of machining parameters of AISI 304L stainless steel with the least error method using Taguchi, RSM, and ANN. *Australian Journal of Mechanical Engineering, 23*(3), 538-548. [CrossRef]

[33] Vankanti, V. K., & Ganta, V. (2014). Optimization of process parameters in drilling of GFRP composite using Taguchi method. *Journal of Materials Research and Technology, 3*(1), 35-41. [CrossRef]

[34] Latha, B., Senthilkumar, V. S., & Palanikumar, K. (2011). Influence of drill geometry on thrust force in drilling GFRP composites. *Journal of Reinforced Plastics and Composites, 30*(6), 463-472. [CrossRef]

[35] Rubio, J. C., Abrão, A. M., Faria, P. E., Correia, A. E., & Davim, J. P. (2008). Effects of high speed in the drilling of glass fibre reinforced plastic: Evaluation of the delamination factor. *International Journal of Machine Tools and Manufacture, 48*(6), 715-720. [CrossRef]

[36] Babu, J., Madarapu, A., Sunny, T., & Ramana, M. V. (2022). Multi characteristic optimization of high-speed machining of GFRP laminate by hybrid Taguchi desirability approach. *Materials Today: Proceedings, 58*, 238. 238-243. [CrossRef]

[37] Mohan, N. S., Kulkarni, S. M., & Ramachandra, A. (2007). Delamination analysis in drilling process of glass fiber reinforced plastic composite materials. *Journal of Materials Processing Technology, 186*(1-3), 265-271. [CrossRef]

[38] Shete, H. V., & Sohani, M. S. (2020). Simultaneous optimization of output parameters in HPC drilling using multi response optimization technique with desirability function approach. *World Journal of Engineering, 17*(3), 437-444. [CrossRef]

[39] Nayak, B. B., Kundu, S., Kumar, M., Kumar, V., Kumar, R., & Shivam, K. P. (2021). Parametric optimization in drilling of GFRP composites using desirability function integrated simulated annealing approach. *Materials Today: Proceedings, 44*, 1983-1987. [CrossRef]

[40] Arslane, M., Slamani, M., Elhadi, A., & Amroune, S. (2024). Multi-response optimization of drilling parameters in hybrid natural fiber composites using Taguchi and desirability function analysis (DFA). *International Journal of Advanced Manufacturing Technology, 135*(11), 5631-5645. [CrossRef]

[41] Shyha, I., Soo, S. L., Aspinwall, D., & Bradley, S. (2010). Effect of laminate configuration and feed rate on cutting performance when drilling holes in carbon fibre reinforced plastic composites. *Journal of Materials Processing Technology, 210*(8), 1023-1034. [CrossRef]

[42] Murakami, D., Okamura, K., Meguro, K., & Shimada, H. (2014). The technical trend and the future of super hard material cutting tools. *Structure, 2*, 1-5.

Journal of Advances in Manufacturing Engineering
Web page info: https://jame.yildiz.edu.tr
DOI: 10.14744/ytu.jame.2026.00003

Original Article

# Fused deposition modeling (FDM) process parameter optimization for PLA component manufacturing

**Serhat MUSTAFA[*1], Dilek MURAT[2], Agah UĞUZ[3], Mustafa Cemal ÇAKIR[3]**

[1]*YAZAKI Systems Technologies, Bursa, Türkiye*
[2]*Department of Econometrics, Bursa Uludağ University, Faculty of Economics and Administrative Science, Bursa, Türkiye*
[3]*Department of Mechanical Engineering, Bursa Uludağ University, Faculty of Engineering, Bursa, Türkiye*

## ARTICLE INFO

*Article history*
Received: 10 March 2026
Revised: 31 March 2026
Accepted: 07 April 2026

**Key words:**
Fused deposition modelling, G-code parameters selection, PLA optimization, S/N proportion, Taguchi method.

## ABSTRACT

Technological developments in manufacturing have significantly improved living standards in recent years. These advancements are largely driven by progress in material science and the development of manufacturing techniques that enable cost-effective mass production. Additive manufacturing (AM) is a production method that creates objects by adding material layer by layer based on three-dimensional model data. In this process, a physical product is generated directly from a 3D Computer-Aided Design (CAD) model. The main objective of additive manufacturing technologies is to produce components with minimal cost, high quality, and optimal efficiency. In this study, the effects of process parameters on the strength, filament consumption, and printing time of PLA (Polylactic Acid) parts produced by Fused Deposition Modelling (FDM) were investigated. The produced parts were 'Clip Control Fixtures (CCF)' used to check the presence of clips on wire harness bundles manufactured at YAZAKI. Wall line count (WLC), infill density (ID), and print speed (PS) were selected as process parameters. Experiments were conducted using the Taguchi L9 experimental design with three levels for each factor. According to the analysis performed under the "larger is better" assumption, WLC had the greatest effect on strength 56.21%, followed by ID 33.49%. The optimal parameter combination for maximum strength was determined as WLC 6, ID 90, and PS 40. For filament consumption "smaller is better", ID showed the highest influence 95.68%. For printing time, PS 71.53% and ID 27.71% were the most influential factors, and the optimal combination was WLC 2, ID 20, PS 120.

**Cite this article as:** Mustafa, S., Murat, D., Uğuz, A., & Çakır, M. C. (2026). Fused deposition modeling (FDM) process parameter optimization for PLA component manufacturing. *J Adv Manuf Eng*, 7(1), 21–30.

## INTRODUCTION

Fused deposition modelling (FDM) is one of the most widely used additive manufacturing (AM) techniques because of its accessibility, relatively low cost, and compatibility with various thermoplastic materials such as polylactic acid (PLA). Despite its advantages, the mechanical performance, material consumption, and production time of FDM-printed parts are strongly influenced by process parameters. Therefore, finding relationships and optimization of these parameters is essential to achieve components with adequate strength, reduced material usage, and efficient production.

In industrial applications, particularly in the automotive sector, fixtures produced by AM method can play an important role in inspection and assembly processes. In

***Corresponding author.**
*E-mail address: serhat.mustafa@yazaki-europe.com

this context, this study focuses on the finding of optimization proportion criteria of process parameters to produce PLA-based CCF used to verify the presence of clips on wire harness bundles manufactured at YAZAKI. WLC, ID, and PS were selected as key process parameters and investigated using the Taguchi L9 experimental design.

Numerous studies in the literature on FDM methodology indicate that process parameters have significant individual effects on production time, filament consumption, and the mechanical strength of printed parts. In particular, the selection of G-code parameters is considered a critical factor in the manufacturing process. Several studies have investigated the influence of G-code parameters on PLA, a sustainable thermoplastic polyester widely used in FDM technology due to its biodegradability, ease of printing, and relatively good mechanical properties. These parameters, however, may also vary depending on the specific filament type used in the printing process. A review of the literature shows that the generated G-code is strongly influenced by parameters such as wall line count, infill density, layer height, and print speed [1]. These parameters have been identified as some of the most influential factors in determining the final performance, material usage, and production efficiency of FDM-printed components.

In a study conducted by Mazlan and Anas, the effects of infill density, wall perimeter, and layer height on the manufacturing performance of 3D printed parts were investigated [1]. The study revealed that the quality and mechanical performance of 3D printed components are influenced not only by the material used but also by specific printing parameters. Both computational analysis and experimental results demonstrated that increasing the values of the three parameters wall perimeter, infill density, and layer height can lead to an improvement in the tensile flexibility of the printed component. It was also concluded that reducing the infill density decreases the cross-sectional area of the structure, which may result in a smaller load-bearing surface area required to maintain structural integrity. Furthermore, increasing the layer height was found to reduce the total printing time; however, this improvement in production efficiency may lead to a rougher and less uniform surface texture in the printed part. These findings highlight the importance of optimizing key printing parameters to balance mechanical performance, production efficiency, and surface quality in FDM-based AM processes.

Furthermore, various other factors can also influence the mechanical properties of FDM-printed components. Lee and Yin conducted a study to investigate the effect of compressed air cooling in a PLA-based FDM 3D printing process [2]. The authors proposed the development of a novel autonomous compressed air-cooling system integrated with the print head. In this system, the airflow direction is controlled through an adjustable fan speed mechanism to directly cool the extruded material during the printing process. This approach also provides improved environmental stability within the printing chamber by facilitating air circulation. The experiments were conducted under constant printing conditions, including 100% infill density, a build platform temperature of 45°C, a nozzle temperature of 210°C, and a printing speed of 30 mm/s. According to the findings of the study, an inverse relationship was observed between the cooling air flow rate and both the dimensional accuracy and mechanical strength of the printed parts. Increasing the airflow rate improved the dimensional quality of the printed components; however, it resulted in a reduction in their mechanical strength. These results indicate that cooling conditions play a significant role in determining the final mechanical and dimensional performance of FDM-produced parts.

Another related study conducted by Yu carries out investigation and examining the effects of layer height, infill density, and print speed on the tensile and compressive properties of PLA materials [3]. In this research, an orthogonal experimental design was employed to effectively minimize the number of required tests while maintaining reliable analytical results. The parameters included variable layer heights (0.15 mm, 0.20 mm, 0.25 mm, and 0.30 mm), infill densities (40%, 60%, 80%, and 100%), and print speeds (30 mm/s, 40 mm/s, 50 mm/s, and 60 mm/s). A total of 16 experiments were conducted using different combinations of these manufacturing parameters. The results of the study indicated that layer height had the most significant influence on the tensile strength of the printed components. However, the G-code parameter settings in this approach were not adequate for the effect of other parameters for output variables.

Unlike the previously mentioned studies, Kartal investigated the effects of surface roughness on PLA material by considering parameters such as bed temperature, nozzle temperature, and layer height using the Taguchi optimization approach [4]. In this study, a Taguchi L9 experimental design was employed, where cubic specimens were printed and their surface roughness values were subsequently measured. During the analysis, the "smaller is better" criterion was adopted, and the average surface roughness value was selected as the response parameter. According to the findings of the study, nozzle temperature was identified as the most influential parameter with an effect ratio of 86.85%, followed by layer height with 7.1% and bed temperature with 5.9%. Based on the experimental results, the author concluded that the optimal parameter combination for improving dimensional accuracy and reducing surface roughness consisted of a bed temperature of 50°C, a nozzle temperature of 230°C, and a layer height of 200 μm. However, it was also emphasized that these parameter settings may not be universally applicable to other 3D printers due to temperature fluctuations within the printer chamber, which can influence the thermal stability of the printing process. In addition to the analysis above, AM technology enables the production of complex prototype components by adjusting various process parameters such as PS, temperature, infill pattern and other printing conditions. Also, the effectiveness of standard G-code parameters, FDM technology also provides the option to select different infill patterns, which can significantly influence the mechanical behavior of printed parts. In this context, Tran conducted a study to investigate how the selection of infill patterns and layer

thickness affects the mechanical strength of PLA materials in 3D printing processes [5]. In this research, nine experimental configurations were evaluated using the Taguchi L9 experimental design. The study considered three different infill patterns zigzag, triangular, and grid as well as three-layer thickness values (0.20 mm, 0.10 mm, and 0.15 mm) as the primary process variables. In total, 27 tensile test specimens were produced in accordance with the ASTM D638 Type IV standard, with three replicates for each experimental condition. The results indicated that the triangular infill pattern provided the highest mechanical strength among the tested configurations, while the zigzag infill pattern resulted in the lowest mechanical performance. These findings demonstrate that the selection of infill pattern and layer thickness plays an important role in determining the mechanical properties of PLA components manufactured using FDM technology.

The performance and efficiency of components produced by 3D printing technologies are strongly influenced by process related factors such as mechanical strength, printing time, and filament consumption. These parameters are critical not only for ensuring structural integrity but also for achieving cost-effective and time-efficient manufacturing. Despite extensive research on FDM-printed PLA parts, existing studies predominantly focus on standardized test specimens and often evaluate performance metrics individually, rather than considering functional components.

However, industrial applications such as CCF require simultaneous consideration of both mechanical performance and production efficiency. In particular, the combined effects of WLC, ID, and PS, especially the role of WLC in load-bearing behavior have not been sufficiently investigated for such applications. Furthermore, achieving a balance between tensile strength, production time, and material consumption remains a key challenge in functional component design.

To address this gap, the present study focuses on the optimization of WLC, ID, and PS parameters for CCF applications using the Taguchi method. Unlike conventional approaches, this work evaluates multiple performance outputs, including mechanical strength, production time, and filament consumption, within a unified framework to identify the most efficient parameter combination. By targeting functional CCF components rather than relying solely on standardized specimens, this study provides a practical and application-oriented contribution to the field. The results offer actionable insights into in-house production and support the development of optimized AM strategies for industrial fixture design.

The main contribution of this study lies in revealing the critical influence of WLC on the mechanical performance of functional CCF components, while simultaneously considering production related outputs within a unified evaluation approach.

**FDM 3D Printing Process Workflow**

The steps involved in the 3D printing process can be defined sequentially as follows. First, the three-dimensional model of the object to be produced is designed and digitally generated using CAD software or obtained through 3D scanning. The created or scanned model is then converted into a file format suitable for slicing software and saved accordingly. In the next stage, the G-code parameters required for the manufacturing process such as material type, layer thickness, ID, and printing temperature are determined. The model is subsequently processed in the slicing software, where it is divided into layers and the corresponding G-code instructions are generated.

The generated G-code is then transferred to the 3D printer. After the printer is prepared for operation, the printing process is initiated, and the physical object is produced layer by layer. Finally, the printed object is removed from the printer, support structures are cleaned if present, and necessary post-processing operations are applied to obtain the final product.

**G-Code Structure and Its Importance in AM**

G-code is a programming language consisting of G and M commands that define machine movements and operations in AM systems. It is automatically generated by slicing software during the conversion of digital models into printable formats and serves as the instruction set guiding the 3D printing process. Acting as a bridge between digital design and physical production, G-code controls key parameters such as toolpath, movement speed, and material extrusion. Furthermore, a fundamental understanding of G-code enables enhanced process control, allowing users to optimize printing performance and effectively troubleshoot potential issues.

**The Effects of G-Code Parameters**

***Wall line count***

WLC, also referred to as the number of perimeters or outer walls, is an important parameter in FDM 3D printing that directly affects the structural strength and durability of printed components. This parameter determines how many solid contour lines are printed around the outer boundary of each layer. Increasing the WLC results in thicker outer shells, which can significantly improve the mechanical strength, stiffness, and overall structural integrity of the printed part. In many cases, higher WLC contributes more to the mechanical performance of a component than ID, since the outer walls typically bear a greater portion of the applied loads. However, increasing the number of wall lines also leads to higher material consumption and longer printing times. Therefore, selecting an appropriate WLC is essential to balance mechanical performance, material efficiency, and production time in FDM manufacturing processes.

***Print speed***

Studies examining the effect of PS on FDM-printed PLA samples have shown that increasing the PS can negatively affect several mechanical and physical properties of the printed components. It has been reported that an increase in PS leads to a reduction in mass, top surface hardness, and

tensile strength, while simultaneously increasing the porosity of the printed structure. In addition, the effective Young's modulus of PLA material decreases after printing, and this reduction becomes more pronounced as the printing speed increases [6]. These findings indicate that PS plays a critical role in determining the mechanical performance and structural integrity of FDM-produced parts.

***Cooling fan***

The dimensional quality and mechanical properties of FDM-printed parts are also influenced by the cooling fan used during the printing process. Research has shown that there is an inverse relationship between the cooling air flow rate and both the dimensional accuracy and mechanical strength of the printed components. A higher cooling airflow rate improves dimensional quality by stabilizing the printed layers; however, it may reduce the mechanical strength of the printed parts [6]. Therefore, optimizing the cooling conditions is essential to achieve a balance between dimensional accuracy and mechanical performance.

***Infill density***

ID has a significant influence on the tensile strength of 3D printed PLA specimens. Independence of the selected infill pattern, an increase in ID has been shown to considerably improve the tensile strength of PLA parts produced using FDM technology. Higher infill densities increase the internal material volume of the structure, resulting in improved load-bearing capacity and enhanced mechanical performance of the printed components.

***Infill pattern***

In addition to ID, FDM G-code parameters also include the option to select different infill patterns. Various infill pattern types exist, and their selection can significantly influence the mechanical properties of printed components. In the study titled "Investigation of the Effect of Infill Pattern and Layer Thickness on the Mechanical Strength of PLA Material in 3D Printing Technology," several commonly used infill patterns were analyzed [7]. Among the evaluated patterns, the triangular infill pattern provided the highest mechanical strength, whereas the zigzag pattern exhibited the lowest mechanical performance. The grid infill pattern forms a lattice structure consisting of intersecting perpendicular lines that create a mesh-like pattern within the printing area. This pattern provides moderate strength while using a relatively small amount of material. Due to this balance between material usage and structural strength, the grid pattern is commonly preferred for functional prototypes and objects subjected to light mechanical loads, and it is also suitable for faster 3D printing applications.

Within the scope of this study, certain G-code-related printing parameters were intentionally kept constant to establish a controlled experimental environment and to ensure a reliable evaluation of the selected variables. These fixed parameters include layer height, nozzle diameter, infill pattern, and cooling conditions as detailed in the following section.

## MATERIALS AND METHODS

**Experimental Procedure**

PLA filament supplied by KIMYA was used in all experiments. Considering the hygroscopic nature of PLA, the material was stored under controlled conditions prior to printing in order to minimize moisture absorption and ensure process stability. All specimens were manufactured using a closed-chamber FDM system BCN3D Epsilon W27 under controlled environmental conditions of approximately 24°C ambient temperature and 40% relative humidity. These conditions were maintained throughout the experiments to reduce moisture-related variability and improve reproducibility.

In addition, to establish a controlled experimental framework, several process parameters were kept constant. The build plate temperature was maintained at 50 °C and the printing temperature was fixed at 200 °C for all experimental runs to ensure consistency. A triangular infill pattern, which has been reported to provide high mechanical strength, was used in all prints. The layer height was set to 0.2 mm, and a 0.4 mm brass nozzle was employed throughout the experiments. The cooling fan speed was fixed at 80% to achieve a balance between sufficient material solidification and stable interlayer bonding. Excessive cooling may weaken interlayer adhesion, whereas insufficient cooling can lead to dimensional inaccuracies; therefore, an intermediate value was selected to ensure consistent printing conditions.

Furthermore, the build orientation was carefully selected to minimize the need for support structures while ensuring that the clip mounting surface remained on the upper side. This configuration was preferred to reduce surface-induced dimensional deviations and maintain assembly tolerances during clip installation. By controlling these parameters, the influence of external factors was minimized, allowing a focused evaluation of the primary process variables, namely WLC, ID, and PS.

The experimental procedure developed within the scope of this study consists of six main stages, designed to systematically determine the optimal process parameters affecting the mechanical properties, filament consumption, and production time of PLA specimens produced via the FDM process.

I. A comprehensive literature review was conducted to identify the key process parameters affecting FDM printing performance. Based on this review, the input parameters and their corresponding levels were determined.
II. A tensile test specimen was designed in SolidWorks according to the ASTM D638 Type I standard. The designed model was then converted into STL format, which is required for the slicing process.
III. Based on the parameter combinations determined using the Taguchi experimental design method, G-code files were generated using the Stratos slicing software.
IV. The generated G-code files were printed using a BCN3D Epsilon W27 3D printer. During the printing process,

output parameters such as filament consumption (m) and printing time (minutes) were recorded.

V. A total of 27 specimens, consisting of three repetitions for each experimental condition, were subjected to tensile testing using a UVE (MNR050) Universal Testing Machine at a crosshead speed of 5mm/min.

VI. The experimental results obtained were analyzed using the Taguchi method, and ANOVA was performed to evaluate the significance of the process parameters.

Accordingly, the input process parameters considered in this study WLC, ID, and PS which are summarized in Table 1. In line with the Taguchi experimental design, each parameter was evaluated at three different levels WLC (2, 4, and 6), ID (20%, 50%, and 90%), and PS (40, 80, 120 mm/s) to determine the optimal combination for improved performance.

There is various testing methods used to evaluate the properties of different types of plastics. Among these, ASTM D638 is one of the most widely used standards for determining the tensile properties of plastic materials. This test is performed by applying a tensile force to a specimen and analyzing various characteristics of the material under stress. The ASTM D638 standard consists of five different specimen specifications. Within the scope of this study, the ASTM D638 Type I tensile test specimen which is shown in Figure 1 was selected because it allows for a more effective analysis of the influence of ID, which was chosen as one of the input parameters in the experimental design.

A tensile test is a fundamental materials science test in which a specimen is subjected to uniaxial tensile forces until fracture occurs. The results obtained from this test are commonly used for material selection in engineering applications, quality control, and predicting how materials will behave under different loading conditions. Tensile strength is defined as the maximum tensile stress that a material can withstand before failure or fracture. This stress corresponds to the highest stress value observed in the stress–strain diagram and is calculated using the following Equation (1):

$$\sigma_t = \frac{F_{max}}{A_0}$$

where $F_{max}$ represents the maximum applied force and $A_0$ denotes the initial cross-sectional area of the specimen.

According to the Taguchi L9 experimental design, tensile tests were conducted on a total of 27 specimens, grouped into sets of three for each parameter combination. The tests were performed using a UVE MNR050 universal testing machine with a capacity of 50 kN, at a constant crosshead speed of 5 mm/min. The experimental setup and testing configuration are illustrated in Figure 2, while the fractured specimens obtained after testing are presented in Figure 3.

**Experimental Results**

The experimental results, including mechanical strength, filament consumption, and production time, were systematically recorded and prepared for further analysis.

**Table 1.** Process input factors algorithms

| Items | Specimen quantity | Input parameters | | |
|---|---|---|---|---|
| | | Wall line count | Infill density (%) | Print speed (mm/s) |
| A1 | 3 | 2 | 20% | 40 |
| A2 | | 2 | 20% | 40 |
| A3 | | 2 | 20% | 40 |
| B1 | 3 | 2 | 50% | 80 |
| B2 | | 2 | 50% | 80 |
| B3 | | 2 | 50% | 80 |
| C1 | 3 | 2 | 90% | 120 |
| C2 | | 2 | 90% | 120 |
| C3 | | 2 | 90% | 120 |
| D1 | 3 | 4 | 20% | 80 |
| D2 | | 4 | 20% | 80 |
| D3 | | 4 | 20% | 80 |
| E1 | 3 | 4 | 50% | 120 |
| E2 | | 4 | 50% | 120 |
| E3 | | 4 | 50% | 120 |
| F1 | 3 | 4 | 90% | 40 |
| F2 | | 4 | 90% | 40 |
| F3 | | 4 | 90% | 40 |
| G1 | 3 | 6 | 20% | 120 |
| G2 | | 6 | 20% | 120 |
| G3 | | 6 | 20% | 120 |
| H1 | 3 | 6 | 50% | 40 |
| H2 | | 6 | 50% | 40 |
| H3 | | 6 | 50% | 40 |
| I1 | 3 | 6 | 90% | 80 |
| I2 | | 6 | 90% | 80 |
| I3 | | 6 | 90% | 80 |

The tensile test results provide detailed insight into the mechanical performance of the specimens. As presented in Table 2, key parameters such as maximum force (N), strain (%), tensile strength (MPa), and elastic modulus (MPa) were obtained. These mechanical properties enable a comprehensive evaluation of the structural behavior of the printed specimens under tensile loading.

In addition to the mechanical properties, process related outputs, including filament consumption and print-

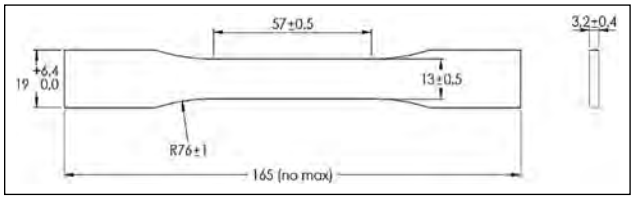


**Figure 1**. ASTM D638 type 1 - tensile test specimen.

**Figure 2**. UVE MNR050 tensile test machine.

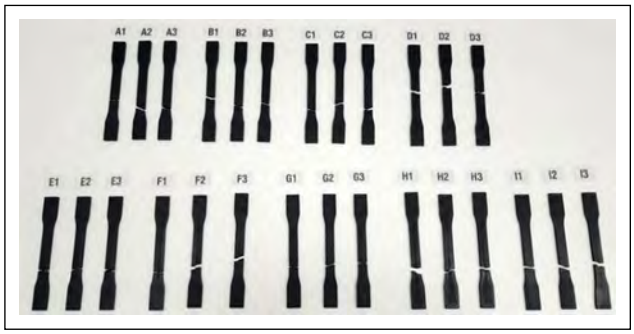

**Figure 3**. Tensile test specimens.

ing time, were also measured. The complete set of output data, combining both mechanical and production-related parameters, is summarized in Table 3. This data set forms the basis for subsequent statistical analysis, including S/N ratio evaluation and ANOVA, as well as optimization using the Taguchi method.

Based on experimental tests, and subsequent analyses, the obtained data were systematically compiled. These output parameters were further analyzed using signal-to-noise (S/N) ratios and ANOVA to identify the most influential factors.

## KEY FINDINGS

In experimental results, Taguchi introduced a performance evaluation criterion known as the signal-to-noise (S/N) ratio, which is used as an analysis variable to assess the robustness and quality of experimental results.

Several assumptions are considered in the calculation of the S/N ratio, including "smaller is better," "nominal is best," and "larger is better." Regardless of the selected assumption, the primary objective in all cases is to maximize the S/N ratio in order to achieve optimal performance and minimize variability.

The findings obtained from the output parameters were evaluated in terms of mechanical strength, filament consumption, and printing time. The experimental results were analyzed based on the appropriate S/N ratio

**Table 2.** Tensile test findings

| Specimen | Fmax (N) | E (MPa) | σt (MPa) | ε (%) |
|---|---|---|---|---|
| A1 | 1844.641 | 2627.867 | 42.069 | 4.526 |
| A2 | 1858.904 | 2612.023 | 41.753 | 2.563 |
| A3 | 1901.203 | 2651.828 | 42.704 | 2.135 |
| B1 | 2011.918 | 2998.894 | 43.948 | 2.828 |
| B2 | 1831.357 | 2837.927 | 39.715 | 1.660 |
| B3 | 2031.600 | 2905.050 | 44.025 | 2.342 |
| C1 | 2301.954 | 3595.173 | 48.554 | 1.708 |
| C2 | 2325.173 | 3581.178 | 49.018 | 3.174 |
| C3 | 2311.136 | 3540.039 | 48.477 | 1.779 |
| D1 | 2062.948 | 2924.634 | 44.978 | 1.900 |
| D2 | 2134.676 | 3048.559 | 47.793 | 2.023 |
| D3 | 2199.706 | 3000.864 | 49.685 | 3.377 |
| E1 | 2164.256 | 3069.198 | 47.258 | 3.637 |
| E2 | 2102.350 | 3133.051 | 46.481 | 2.967 |
| E3 | 2176.825 | 3127.246 | 47.981 | 3.348 |
| F1 | 2733.224 | 3981.620 | 59.161 | 2.676 |
| F2 | 2826.929 | 3983.078 | 61.858 | 4.089 |
| F3 | 2670.678 | 3968.812 | 58.228 | 1.712 |
| G1 | 2235.871 | 3124.262 | 48.152 | 1.853 |
| G2 | 2309.029 | 3165.595 | 49.550 | 2.325 |
| G3 | 2352.569 | 3162.160 | 50.716 | 2.363 |
| H1 | 2824.032 | 3884.153 | 64.057 | 2.726 |
| H2 | 2847.627 | 4143.654 | 65.323 | 2.104 |
| H3 | 2779.362 | 3919.540 | 63.233 | 5.392 |
| I1 | 3082.907 | 4269.855 | 67.368 | 2.210 |
| I2 | 3125.733 | 4343.747 | 68.386 | 2.357 |
| I3 | 3152.791 | 4466.904 | 69.105 | 2.961 |

criteria corresponding to each output parameter. According to the ANOVA results, WLC was identified as the most statistically significant factor affecting tensile strength, with the highest contribution ratio. In contrast, ID and PS showed greater influence on production time and material consumption. The statistical analysis confirms that WLC plays a dominant role in mechanical performance, while ID and PS are more critical in terms of manufacturing efficiency.

### Analysis of Strength, Material Consumption and Time

#### *Strength*

In this study, higher strength values were considered as an indicator of better-quality performance. Accordingly, the system was optimized based on the "larger is better" assumption in the Taguchi analysis. According to these findings, the highest S/N ratios were obtained at the following factor levels:

- For the WLC factor, the highest effect was observed as 6 with a contribution ratio of 56.21%.

**Table 3.** Process output findings

| Item | Specimen quantity | Output parameters | | | |
|---|---|---|---|---|---|
| | | Tensile strength (Mpa) | Average of tensile strength (mpa) | Filament consumption (meters) | Time (min) |
| A1 | 3 | 42.069 | 42.175 | 0.776 | 28 |
| A2 | | 41.753 | | 0.776 | 28 |
| A3 | | 42.704 | | 0.776 | 28 |
| B1 | 3 | 43.948 | 42.563 | 0.993 | 21.33 |
| B2 | | 39.715 | | 0.993 | 21.33 |
| B3 | | 44.025 | | 0.993 | 21.33 |
| C1 | 3 | 48.554 | 48.683 | 1.276 | 22.33 |
| C2 | | 49.018 | | 1.276 | 22.33 |
| C3 | | 48.477 | | 1.276 | 22.33 |
| D1 | 3 | 44.978 | 47.485 | 0.836 | 17.33 |
| D2 | | 47.793 | | 0.836 | 17.33 |
| D3 | | 49.685 | | 0.836 | 17.33 |
| E1 | 3 | 47.258 | 47.240 | 1.03 | 17.66 |
| E2 | | 46.481 | | 1.03 | 17.66 |
| E3 | | 47.981 | | 1.03 | 17.66 |
| F1 | 3 | 59.161 | 59.749 | 1.28 | 48 |
| F2 | | 61.858 | | 1.28 | 48 |
| F3 | | 58.228 | | 1.28 | 48 |
| G1 | 3 | 48.152 | 49.473 | 0.893 | 14.667 |
| G2 | | 49.55 | | 0.893 | 14.667 |
| G3 | | 50.716 | | 0.893 | 14.667 |
| H1 | 3 | 64.057 | 64.204 | 1.067 | 40 |
| H2 | | 65.323 | | 1.067 | 40 |
| H3 | | 63.233 | | 1.067 | 40 |
| I1 | 3 | 67.368 | 68.286 | 1.286 | 28 |
| I2 | | 68.386 | | 1.286 | 28 |
| I3 | | 69.105 | | 1.286 | 28 |

**Table 4.** Anova results for strength

| Source | Means of S/N ratios Levels | | | DF | Seq SS | Adj MS | Fac eff (%) | F | p |
|---|---|---|---|---|---|---|---|---|---|
| | 1 | 2 | 3 | | | | | | |
| WLC | 32.94 | 34.18 | 35.58 | 2 | 10.40 | 5.20 | 56.21 | 30.27 | 0.03 |
| ID | 33.31 | 34.07 | 35.32 | 2 | 6.20 | 3.10 | 33.49 | 18.04 | 0.05 |
| PS | 34.73 | 34.27 | 33.71 | 2 | 1.56 | 0.78 | 8.45 | 4.55 | 0.18 |
| Res. Err. | | | | 2 | 0.34 | 0.17 | 1.86 | | |
| Total | | | | 8 | 18.51 | | 100 | | |

DF: Degrees of freedom; Seq SS: Sum square; Adj MS: Adjusted mean square; Fac. eff: Factor effect; Res. Err.: Residual error.

- For the ID factor, the highest effect was observed as 90% with a contribution ratio of 33.49%.
- For the PS factor, the highest effect was observed as 40 mm/s with a contribution ratio of 8.45%.

These results indicate that the WLC parameter has the most significant influence on the tensile strength, followed by ID and PS according to Anova results in Table 4.

**Table 5.** Anova results for filament consumption

| Source | Means of S/N ratios Levels | | | DF | Seq SS | Adj MS | Fac eff (%) | F | p |
|---|---|---|---|---|---|---|---|---|---|
| | 1 | 2 | 3 | | | | | | |
| WLC | 0.05 | -0.28 | -0.59 | 2 | 0.61 | 0.30 | 2.80 | 3.59 | 0.22 |
| ID | 1.58 | -0.25 | -2.15 | 2 | 20.86 | 10.43 | 95.68 | 122.96 | 0.01 |
| PS | -0.17 | -0.19 | -0.46 | 2 | 0.16 | 0.0 | 0.75 | 0.96 | 0.51 |
| Res. Err. | | | | 2 | 0.17 | 0.08 | 0.78 | | |
| Total | | | | 8 | 21.80 | | 100 | | |

DF: Degrees of freedom; Seq SS: Sum square; Adj MS: Adjusted mean square; Fac. eff: Factor effect; Res. Err.: Residual error.

**Table 6.** Anova results for printing time

| Source | Means of S/N ratios Levels | | | DF | Seq SS | Adj MS | Fac eff (%) | F |
|---|---|---|---|---|---|---|---|---|
| | 1 | 2 | 3 | | | | | |
| WLC | -27.50 | -27.78 | -28.10 | 2 | 0.55 | 0.27 | 0.58 | 3.27 |
| ID | -25.68 | -27.85 | -29.85 | 2 | 26.05 | 13.02 | 27.71 | 155.56 |
| PS | -31.54 | -26.77 | -25.08 | 2 | 67.25 | 33.62 | 71.53 | 401.60 |
| Res. Err. | | | | 2 | 0.17 | 0.08 | 0.18 | |
| Total | | | | 8 | 94.01 | | 100 | |

DF: Degrees of freedom; Seq SS: Sum square; Adj MS: Adjusted mean square; Fac. eff: Factor effect; Res. Err.: Residual error.

**Material Consumption**

Minimizing filament consumption was considered an important performance criterion. Therefore, the system was optimized based on the "smaller is better" assumption in the Taguchi analysis. According to these findings, the highest S/N ratios were obtained at the following factor levels shown in Table 5:

- For the WLC factor, the highest effect was observed as 2 with a contribution ratio of 2.80%.
- For the ID factor, the highest effect was observed as 20% with a contribution ratio of 95.68%.
- For the PS factor, the highest effect was observed as 40 mm/s with a contribution ratio of 0.75%.

These results indicate that the ID parameter has the most significant influence on filament consumption, while the effects of WLC and PS are relatively limited.

**Printing Time**

Minimizing the printing time was considered an important objective to improve production efficiency. Therefore, the system was optimized based on the "smaller is better" assumption in the Taguchi analysis. The ANOVA results obtained using the time variable are presented in the corresponding table. According to these findings, the highest S/N ratios were obtained at the following factor levels:

- For the WLC factor, the highest effect was observed as 2 with a contribution ratio of 0.58%.
- For the ID factor, the highest effect was observed as 20% with a contribution ratio of 27.71%.
- For the PS factor, the highest effect was observed as 120 with a contribution ratio of 71.53%.

These results indicate that the PS parameter has the most significant influence on printing time, followed by ID, while the effect of WLC is relatively limited illustrated in S/N ratios shown in Table 6 below.

## RESULTS AND DISCUSSION

The Taguchi-based optimization results indicate that WLC is the most influential parameter governing tensile strength, whereas ID, and PS predominantly affect production time and material consumption. This can be attributed to the fact that WLC directly determines the number of outer perimeters, thereby enhancing load-bearing capacity and interlayer bonding strength. In contrast, ID and PS mainly influence the internal structure and deposition rate, which are more closely associated with manufacturing efficiency rather than structural reinforcement.

Beyond their individual contributions, a notable synergistic interaction between ID and PS was identified. At elevated PS values, the reduced residence time of extruded material limits interlayer diffusion, leading to inadequate bonding and the formation of internal voids. This effect becomes more critical at lower ID levels, where the reduced material density amplifies structural discontinuities. Conversely, higher ID values can partially mitigate the adverse effects of increased PS by improving internal support and reducing porosity. These findings highlight that the combined influence of PS and ID plays a decisive role in balancing mechanical performance and internal integrity.

The observed reduction in tensile performance at higher PS values can be further explained by increased porosi-

ty formation. As the printing speed increases, insufficient bonding between adjacent filaments leads to micro-voids, which act as stress concentration sites and initiate premature failure under tensile loading. This behavior is consistent with the fundamental characteristics of FDM processes, where interlayer adhesion is strongly dependent on thermal diffusion and bonding time.

Although tensile testing was conducted using standard specimens, the selected geometry and loading conditions were designed to represent the critical mechanical behavior of CCFs. In real applications, CCF components are exposed to localized stresses and repetitive mechanical interactions, where both strength and structural integrity are essential. Therefore, the obtained results provide a representative and practically relevant basis for evaluating the performance of CCFs under operational conditions.

The interpretation of these findings should be considered within the constraints of the experimental setup. All experiments were conducted using a single material type PLA brand name is called KIMYA, which may limit the generalizability of the results to other thermoplastics with different thermal and rheological properties. Furthermore, the experiments were carried out on a closed-chamber FDM system on BCN3D Epsilon W27 3D Printer machine and under controlled environmental conditions approximately 24°C ambient temperature and 40% relative humidity. Such conditions can significantly influence cooling behavior, interlayer adhesion, and dimensional stability, and may lead to different outcomes in open-frame systems or varying environmental conditions for reporoducibility.

In addition, several process parameters were kept constant, including a layer height of 0.2 mm, a brass nozzle diameter of 0.4 mm, and a cooling fan speed of 80%. While this controlled approach enables a focused investigation of WLC, ID, and PS, it restricts the assessment of potential interactions between these fixed parameters and the studied variables. Variations in layer height or cooling conditions, for instance, could alter interlayer bonding mechanisms and consequently affect mechanical performance.

Despite these limitations, this study makes a significant application-oriented contribution by focusing on functional CCF components rather than solely on conventional standardized test specimens. Although the experiments were conducted using standard tensile specimens, the findings are interpreted in the context of real fixture applications. By integrating mechanical strength, production time, and filament consumption into a unified optimization framework, the study provides a comprehensive basis for decision-making in in-house fixture production. Future work should extend this approach by incorporating different materials, printer configurations, and environmental conditions, as well as advanced multi-objective optimization techniques.

## CONCLUSION

This study aims to investigate the effects of process parameters on the strength, filament consumption, and printing time of PLA materials used in the production of fixtures. Within this scope, WLC, ID, and PS were considered as primary process parameters. The experiments were carried out according to the Taguchi L9 experimental design, using a total of 27 specimens, where each factor was evaluated at three different levels.

Based on the calculated signal-to-noise (S/N) ratios, the highest strength value was obtained with the factor level combination of WLC 6, ID 90, and PS 40. For filament consumption, the effect of ID was calculated as 95.68%, while the contribution of WLC was 2.80%, and the optimal combination was determined as WLC 2, ID 20, and PS 40. For the printing time, the results indicated that the most influential factors were PS 71.53% and ID 27.71%, with the optimal parameter combination identified as WLC 2, ID 20, and PS 120.

These findings demonstrate how process parameters influence AM processes using PLA to enhance production efficiency and mechanical performance. Identifying critical factors affecting strength, material consumption, and production time provides valuable insights for improving manufacturing efficiency and product quality.

This study identifies WLC as a key parameter controlling the mechanical performance of CCF components and improving process efficiency. Future studies may focus on different materials, more complex geometries, and tighter tolerances to further advance this field.

**Data Availability Statement**

The authors confirm that the data that supports the findings of this study are available within the article. Raw data that support the finding of this study are available from the corresponding author, upon reasonable request.

**Author's Contributions**

Serhat Mustafa: Conceptualization, Data curation, Investigation, Methodology, Resources, Software, Valid- ation, Visualization, Literature Review, Draft Preparation

Dilek Murat: Data Curation, Formal Analysis, Methodology, Software, Visualization, Draft Preparation

Agah Uğuz: Conceptualization, Data Curation, Investigation, Methodology, Administration, Resources, Supervision, Draft Preparation, Review and Editing

Mustafa Cemal Çakır: Conceptualization, Data Curation, Investigation, Methodology, Administration, Resources, Supervision, Draft Preparation, Review and Editing.

**Conflict of Interest**

The authors declared no potential conflicts of interest with respect to the research, authorship, and/or publication of this article.

**Statement on the Use of Artificial Intelligence**

Artificial intelligence was not used in the preparation of experiments and article states.

**Ethics**

There are no ethical issues with the publication of this manuscript.

## REFERENCES


[1] Mazlan, M.A., Anas, M.A., Nor Izmin, N.A., & Abdullah, A.H. (2023). Effects of Infill Density, Wall Perimeter and Layer Height in Fabricating 3D Printing Products. *Materials, 16*(2), Article 695. [CrossRef]

[2] Lee, C.-Y., & Liu, C.-Y. (2019). The influence of forced-air cooling on a 3D printed PLA part manufactured by fused filament fabrication. *Additive Manufacturing, 25*, 196–203.

[3] Yu, Z., Gao, Y., Jiang, J., Gu, H., Lv, S., Ni, H., Wang X., & Jia C. (2019). Study on Effects of FDM 3D Printing Parameters on Mechanical Properties of Polylactic Acid. *IOP Conference Series: Materials Science and Engineering, 688*, Article 033026. [CrossRef]

[4] Kartal, F. (2017). Optimization of fused deposition modeling process parameters by Taguchi methodology. *International Journal of 3D Printing Technologies and Digital Industry, 1*(1), 49–56. [Turkish]

[5] Cho, E.E., Hein, H.H., Lynn, Z., Hla, S.J., & Tran, T. (2019). Investigation on influence of infill pattern and layer thickness on mechanical strength of PLA material in 3D printing technology. *Journal of Engineering and Science Research, 3*(2), 27–37. [CrossRef]

[6] Kamer, M.S., Temiz, S., Yaykasli, H., Kaya, A., & Akay, O.E. (2022). Effect of printing speed on FDM 3D-printed PLA samples produced using different two printers. *International Journal of 3D Printing Technologies and Digital Industry, 6*(3), 438–448.

[7] Eryıldız, M. (2021). Effect of build orientation on mechanical behavior and build time of FDM 3D-printed PLA parts: an experimental investigation. *European Mechanical Science, 5*(3), 116–120. [CrossRef]

J Adv Manuf Eng, Vol. 7, Issue. 1, pp. 31–43, June, 2026

Journal of Advances in Manufacturing Engineering
Web page info: https://jame.yildiz.edu.tr
DOI: 10.14744/ytu.jame.2026.00004

Original Article

# Comprehensive analysis of large language model capabilities in face milling operations with virtual twin verification

**Uğur ENIŞ, Mehmet Şamil SOYER, Hanife ÜNAL HELVACIOĞLU, Muhammet Mustafa SAVAŞÇI**

*Research and Development, Siemens A.Ş., İstanbul, Türkiye*

## ARTICLE INFO

*Article history*
Received: 12 February 2026
Revised: 20 April 2026
Accepted: 04 May 2026

**Key words:**
Machining, face milling, artificial intelligence, large language models, generative AI.

## ABSTRACT

This paper presents a comprehensive analysis of large language models (LLMs) capabilities in the machine tool domain, specifically focusing on face milling operations. The research evaluates how different prompt techniques (zero-shot, few-shot, and tree-of-thought) affect LLMs' ability to perform tasks traditionally requiring human domain expertise, such as interpreting G-code, recommending appropriate cutting tools, and calculating machining parameters. Performance is evaluated by comparing LLM outputs to industry-standard CAM software and digital twin simulations to verify practical applicability. The findings indicate that current LLM technology shows promise for transforming and optimizing complex engineering tasks in manufacturing but still requires additional operator input and customized approaches to achieve complete operational accuracy. This work contributes to understanding how generative Artificial Intelligence (AI) can be leveraged to optimize, generalize, and standardize machining procedures in industrial applications.

**Cite this article as:** Eniş, U., Soyer, M. Ş., Ünal Helvacıoğlu, H., & Savaşçı, M. M. (2026). Comprehensive analysis of large language model capabilities in face milling operations with virtual twin verification. *J Adv Manuf Eng*, 7(1), 31–43.

## INTRODUCTION

A Large Language Model is a type of artificial intelligence (AI), that is trained with massive amounts of text and purposed to generate humane responses via various natural language processing (NLP) techniques such as, text generation, summarization, and translation. Recent advancements in LLMs have transformed the approach of knowledge share and gathering significantly. Generative AI is also a key value for the machining industry to optimize, generalize and standardize procedures of machining.

In manufacturing, the process of removing unwanted segments of metal workpiece in the form of chips is known as machining. Machining is one of the five groups of manufacturing processes which includes casting, forming, powder metallurgy and joining [1]. The machining process will shape the workpiece as desired, and it is usually done using machine and cutting tools. The machining cutting process can be divided into two major groups which are (i) cutting process with traditional machining (e.g., turning, milling, boring and grinding) and (ii) cutting process with modern machining (e.g., electrical discharge machining (EDM) and abrasive waterjet (AWJ) [2]. Machining processes play a pivotal role in the manufacture of final components, whose outcome, depending on the machining conditions and strategies, can significantly influence the material's functional performances [3].

In recent years, artificial intelligence and machine learning techniques have been increasingly adopted to address various challenges in machining. Soori et al. [4] provided a comprehensive review of machine learning and AI applications in CNC machine tools, covering areas such as

*Corresponding author.
*E-mail address: ugur.enis@siemens.com

process optimization, predictive maintenance, and adaptive control. Similarly, Pimenov et al. [5] critically reviewed AI systems developed specifically for tool condition monitoring, highlighting the potential of data-driven approaches to reduce tool failures and improve machining efficiency. These studies illustrate that AI-based methods have become well-established for specific machining sub-tasks, yet their reliance on structured numerical data and predefined feature engineering limits their generalizability across diverse operational scenarios.

A closely related challenge is the automated selection of cutting tools, which traditionally depends on expert knowledge and catalog-based reasoning. Navaneethan et al. [6] reviewed the state of automated cutting tool selection methods, encompassing rule-based systems, case-based reasoning, and machine learning approaches. Their analysis revealed that despite notable progress, existing methods still struggle to incorporate the breadth of contextual factors — such as workpiece geometry, material properties, and machine constraints — that a human expert naturally considers. This limitation points toward the need for AI systems capable of natural language understanding and multi-factor reasoning.

Traditional machine tool operations involve examining the G-Code, obtaining information about the material to be machined, selecting the appropriate tool for the operation based on this information, and adjusting the federate and spindle speed in accordance with the selected tool material and workpiece material to be machined [7].

These operations represent a set of cognitive tasks that require high knowledge of the discipline in line with the experience of the domain expert. After the transfer of specialized knowledge, training of new personnel, validation of the theoretical knowledge acquired in line with the practices, the capacity and ability to fulfill these tasks are acquired.

However, with LLM technology reaching the capacity to perform cognitive tasks such as natural language understanding, generation, and reasoning, it offers the potential to transform, optimize, and comprehend complex engineering problems for such tasks [8]. Recent research has demonstrated growing interest in applying LLMs to various manufacturing domains. Makatura et al. [9] evaluated LLM capabilities across design and manufacturing tasks, including CNC machining project optimization, revealing both promising performance and notable limitations in spatial reasoning. Ni et al. [10] proposed an LLM-based manufacturing process planning approach aligned with Industry 5.0, utilizing prompt engineering to guide sequential decision-making in process plan generation. In a broader scope, Shahin et al. [11] surveyed the applications of generative AI across the manufacturing lifecycle, documenting case studies in quality control, process optimization, and production planning while identifying critical gaps in domain-specific adaptation. Furthermore, the integration of generative AI with digital twin technology has emerged as a complementary avenue; Mata et al. [12] developed a comprehensive framework combining human expertise with generative AI in digital twin-based manufacturing systems, demonstrating enhanced decision-making capabilities through virtual-physical synchronization.

Within this broader trend, several studies have specifically investigated LLM capabilities for G-code — the standard programming language for CNC machine tools. As noted in the work by Jignasu et al. [13], foundational LLMs showed limited understanding of geometries encoded in G-code for additive manufacturing. Expanding on this direction, Šket et al. [14] compared ChatGPT-3.5 and ChatGPT-4o for G-code generation in CNC machining and found that while newer models produced more accurate code, they still required human verification for practical deployment. Abdelaal et al. [15] addressed this reliability concern by proposing GLLM, a self-corrective G-code generation framework that incorporates user feedback loops to iteratively improve the generated output. These studies collectively establish that while LLMs possess a degree of competence in G-code related tasks, significant challenges remain in ensuring accuracy and completeness.

Beyond G-code generation, researchers have explored LLM deployment for broader CNC operational tasks. Kanimozhi and Sriker [16] demonstrated an explorative deployment of a fine-tuned LLM for on-site CNC machine operator assistance, showing that domain-adapted models can address machine-specific queries more effectively than general-purpose LLMs. Jeon et al. [17] proposed CNC-Talks, a conversational machine monitoring framework that integrates LLMs with real-time data retrieval augmented generation (RAG) to enable natural language-driven interaction with CNC equipment. Stathatos et al. [18] applied LLMs to high-level computer-aided process planning (CAPP) in a distributed manufacturing context, generating alternative process plans from textual part descriptions. While these works demonstrate LLM capabilities in individual aspects of manufacturing, they each focus on a single sub-task rather than evaluating LLMs across the full spectrum of cognitive tasks involved in a machining workflow.

Despite this growing body of research, no study has yet provided a comprehensive evaluation that compares multiple LLMs across different prompt engineering strategies on a complete machining workflow — encompassing G-code interpretation, cutting tool recommendation, and machining parameter estimation — while simultaneously validating the outputs against both industry-standard CAM software and digital twin simulations. In this paper, the domain expertise of foundational LLMs is evaluated across these three key tasks in the machine tool domain to determine whether LLMs can serve as a generic, optimal, and standardized solution for these operations. For this purpose, different foundational LLMs and different prompt techniques will be employed and compared.

## MATERIALS AND METHODS

In this section, the traditional approaches for selecting machine parameters with domain expertise will be examined. The discussion begins with face milling as the reference operation.

**Face Milling**

Face milling is a machining operation that controls the height of the machine part. It is commonly used to generate flat reference surfaces before subsequent finishing operations.

Like all milling operations, face milling employs a cutting tool that rotates while the machined part remains stationary. Face milling requires that a specific amount of material be removed from the top of part, at one or several depth levels, in a single cut or multiple cuts [19].

Based on the machining operation, selection of a face mill cutter must consider several conditions [19].

- CNC machine specifications and condition
- Part material to be machined
- Setup method and work holding integrity
- Method of mounting
- Cutter overall construction
- Face mill diameter
- Number of inserts and insert geometry.

The last two items influenced actual program development at most, because it has a direct relation with the cutting feed and spindle speed. the number of inserts and milling diameter directly affects the cutting speed and spindle speed [20].

**Large Language Models (LLMs)**

Text generation and summarization with LLMs have increased significantly in recent years for many industries. Foundational LLMs which have been open sourced for use by the general have been trained with a large portion of data that includes many different fields including engineering, art, sports, and science. This way, LLMs can be used well for different types of industries and generate text for different types of tasks.

Also with reinforcement learning, the LLMs capabilities went beyond. Reinforcement learning is a learning type based on a rewarding system for the LLMs to gather feedback directly from humans [21]. This enabled chatbots to establish communication based on user feedback and align the results based on the needs.

As concluded in work by Jignasu et al. [13], while foundational LLMs can perform with reasonable proficiency, they also depict their critical limitations. Their experiments have shown that the understanding of LLMs for geometries with given G-Codes were limited in additive manufacturing domain.

**Prompt Engineering**

In this paper, three different types of prompting have been examined. Each type is presented with its role in the machine tool evaluation workflow.

***Zero-Shot Prompts***

Zero-shot prompts refer to instruction based single prompt, that can contain inputs such as:

- Step-by-step guidance
- Options to select
- Question etc.

Task description in a zero shot with instructions plays a crucial role during this type of prompting. E.g. "Translate 'how are you' into German."

As described in the work by Wei [22], a well-constructed zero-shot prompt performs considerably better than others. Theoretically a zero-shot prompt should contain whole information with the instructions for LLM to reason the question, evaluate the data, and format result in an expected format.

***Few-Shot Prompts***

Few-shot prompts generally require a few task related examples that can lead to an optimum solution for the given task. For better understanding of user need, AI can be adjusted in-context via few-shot prompts [23]. This leads to better generations via LLMs.

Few-shot prompting is a procedure that you give examples regarding to task for a better understanding and limit LLM to work based on the subject. It will lead LLM to a solution.

Few-shot prompting acts like a fine-tuning procedure. With prompts, users can define a context for LLM to understand what is needed, described or wanted for user.

***Tree of Thought Prompts***

A chain-of-thought is a series of intermediate natural language reasoning steps that lead to final output [24]. Tree of thoughts prompts are a combination of single-shot and few-shot prompting, it works poorly on tasks that require reasoning abilities and often does not improve substantially with increasing language model scale.

In the work by Wei [24], it is concluded that chain-of-thought prompting is a simple method for enhancing the reasoning capabilities of LLMs. It is understood that, with a chain of thought, LLMs can scale way better for arithmetic, symbolic and commonsense reasoning.

Tree of thought prompt contains instruction and input, and the procedure continues with the requirement of more answers. A self-discussion will be led by the LLM resulting in the perfect scenario for the output.

**Procedures**

The main purpose of this methodological approach is, by using different prompt techniques, to determine to what extent LLMs can effectively perform the tasks mentioned above, which are based on human expertise in the traditional sense. These critical cognitive tasks mostly remain dependent on humans, and LLMs offer a new opportunity to automate these tasks. However, the direct use of outputs can cause situations such as damage to the tool, spoilage of the workpiece, etc., meaning, in terms of practical applicability, verification is needed. Therefore, the methodology includes verification processes by comparing the generated outputs with CAM software (Siemens NX) [25] widely used in the industry and with simulations of the digital twin application (Create MyVirtual Machine) [26] also produced by Siemens for the Sinumerik CNC controller.

To make an evaluation specific to the relevant domain, the following LLM models have been selected. These models provide a balanced comparison across commercial and open-source LLM families.

Claude V3.7 Sonnet: Anthropic' s latest hybrid reasoning model; supports both fast inference and deep thought modes [27].

DeepSeek-R1: DeepSeek's inaugural open-source language model; designed for code and general-purpose tasks with competitive performance across benchmarks. Offers transparency, flexibility, and strong multilingual capabilities [28].

GPT-4.5: OpenAI's transitional model bridging GPT-4 and future iterations. Combines improved reasoning with faster response times and better tool integration. Ideal for both complex problem solving and everyday AI assistance [29].

**Ground Truth Definition**

In this section, the exact dataset ("ground truth") used as a reference in the comparative evaluation of LLM capabilities is defined in detail. Two face milling operations have been examined to compare and give in context.

***Face Milling Operation Example 1***

*Workpiece material and tool features*

The tool configuration for this operation is shown in Figure 1.

Material: C40 Steel (AISI/SAE 1040)
Tool Type: Facing Tool
Tool Diameter: 52 mm
Number of Flutes: 6
Cutting Angle: 45 °

*Spindle speed and feed rate*

Spindle speed for roughing: 980 RPM
Spindle speed for finishing: 1100 RPM
Cutting speed (Vc) for roughing: 160 m/min
Cutting speed (Vc) for finishing: 180 m/min
Feed rate for roughing: 880 mm/min
Feed rate for finishing: 530 mm/min
Feed per Tooth (Fz): 0.08 mm/rev

*Operation Description*

A face-milling operation is performed. It contains two groups, for roughing and finishing. The tool approaches the part along the Z axis to the reference plane (G507(Z20)), then moves in the part to 2.2 mm (G1 Z-2.2) and begins cutting by descending 0.2 mm below the surface (G1 Z-2.0). And then the finishing group starts with going first to the reference plane(G507). Then, finishing starts with going down to cutting area with command (G1 Z-2.5). And face milling operation continues.

*Geometric Description*

Initial setup:

- Program begins with G17 (XY plane), G40 (cutter compensation off), G90 (absolute positioning)
- Tool selection: "ALU_D63" with actual cutting diameter of 52mm and 6 teeth
- Workpiece defined as box shape with dimensions 155x100x20

Approach:

- Rapid traverse (G0) to initial position X5 Y-135
- Spindle starts at S980 rpm with cutting speed VC=160m/min

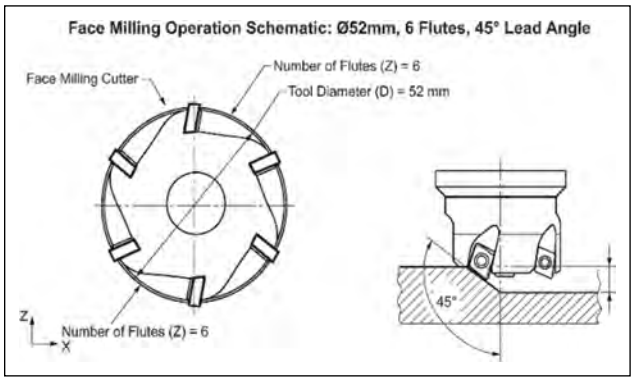


**Figure 1**. Tool scheme for face milling operation example 1.

- Feed rate F880 with feed per tooth FZ=0.15mm
- Rapid descent to Z1mm followed by coolant activation (M8)

Roughing operation:

- Plunge cut to Z-2.2mm with 3mm corner rounding (RNDM=3)
- Zigzag pattern with 31mm step over (AE):
  - Linear move from Y-135 to Y0
  - 2. Step right to X36
  - Linear move to Y-100
  - Step right to X67
  - Linear move to Y0
  - Step right to X98
  - Linear move to Y-100
  - Step right to X129
- Final move to Y0 Retract to Z2mm at end of roughing

Finishing operation:

- Repositioning to X0 Y-135 with increased spindle speed S1100 (VC=180m/min)
- Reduced feed rate F530 (FZ=0.08mm) for better surface finish
- Six parallel vertical passes with 26mm step over (AE):

1. Pass at X0: Cut from Y-135 to Y35, retract to Z2
2. Pass at X26: Cut from Y-135 to Y35, retract to Z2
3. Pass at X52: Cut from Y-135 to Y35, retract to Z2
4. Pass at X78: Cut from Y-135 to Y35, retract to Z2
5. Pass at X104: Cut from Y-135 to Y35, retract to Z2
6. Pass at X130: Cut from Y-135 to Y35, retract to Z2

- Finishing depth Z-2.5mm (0.3mm deeper than roughing)

Surface Coverage:

- X-axis coverage: 0mm to 130mm (total width of 130mm)
- Y-axis coverage: -135mm to 35mm (total length of 170mm)

***Face Milling Operation Example 2***

*Workpiece material and tool features*

The tool configuration for this operation is shown in Figure 2.

Material: Cast iron
Tool Type: Facing Tool
Tool Diameter: 25 mm
Number of Flutes: 3
Cutting Angle: 45 °

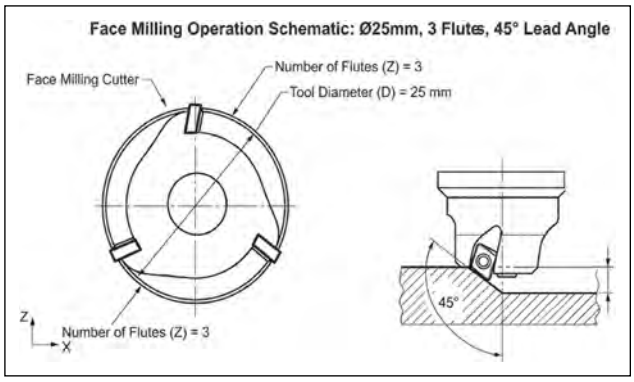


**Figure 2**. Tool scheme for face milling operation example 2.

*Spindle Speed and Feed Rate*
Spindle Speed: 600 RPM
Feed rate: 180 mm/min

*Operation Description*
A face-milling operation is performed. The operation is executed in multiple passes with decreasing depth: 1.5mm, 1.0mm, 0.5mm, and 0.0mm. The tool follows a zigzag pattern with both linear and circular movements. The operation runs at a spindle speed of 600 RPM with a feed rate of 180mm/min. Coolant is active during the cutting operation. The coolant type is emulsion with boron oil.

*Geometric Description*
Initial setup:
- The program begins with G17 (XY plane), G40 (cutter compensation off), G90 (absolute positioning), G94 (feed per minute)
- Tool selection: "MILL_D25" with 25mm cutting diameter
- Program uses G54 workpiece coordinate system
- Approach:
- Initial rapid positioning to X-360 Y223.9
- Tool change and setup with MILL_D25
- Spindle starts at S600 rpm with coolant activation (M8)
- Initial positioning to X-46.138 Y23.724 with B0 and C0

Cutting operation:
- Four identical passes at different Z depths (1.5mm, 1.0mm, 0.5mm, 0.0mm)
- Each pass follows the same pattern:
  - Linear cuts along X-axis
  - Circular interpolation (G2/G3) for curved features
  - Combined linear and circular movements creating a complex profile

Surface coverage:
- X-axis coverage: approximately -49mm to +37mm
- Y-axis coverage: approximately -20mm to +24mm
- Z-axis levels: 1.5mm, 1.0mm, 0.5mm, and 0.0mm

**Prompt Techniques Examined Specific to Machine Tool Domain**

In this section, it is explained in detail how the selected prompt techniques -Zero- Shot, Few- Shot and Tree of Thought- are applied to the tasks in the study. The objective is to show how each technique supports operation review, tool selection, and parameter estimation.

***Role:*** *CNC Machine Tool Expert*
***Instruction:*** *Analyse the below G-Code and extract the operation type and geometric description of the operation.*
***Input:*** *<GCODE>*
***Explanation:*** *<Area for LLM output>*

**Figure 3**. Zero shot prompt template for operation examination.

***Role:*** *CNC Machine Tool Expert*
***Instruction:*** *Analyse the below G-Code and extract operation type and geometric description of the operation.*
***Example:***
*<GCODE_1>, <Explanation of GCODE_1>*
***Input:*** *<GCODE>*
***Explanation:*** *<Area for LLM output>*

**Figure 4**. Few shots prompt template for operation examination.

***Prompt Configurations for Operation Review Task***

The main purpose at this stage is to evaluate the LLM's ability to correctly parse and interpret a universally written G Code part for the Face Milling operation. Thanks to the relevant prompt, it will be asked to infer information such as a specific "Operation Type" (e.g.: Face Milling) and "Geometric Description" (e.g.: the process of correcting a 100x80 mm surface by removing 0.5 mm).

Workpiece material and hardness are defined using general information obtained from factory data. Although this information is not directly used in this stage, it is critical for subsequent tasks and is included in the setup.

***Zero Shot Prompting Application for Direct Inference in Operation Examination Task***

With this prompt technique, it is designed in such a way that the LLM is directly requested to perform a specific task using its general knowledge about CNC machining, G-Code analysis. Within the prompt, a role is usually assigned to the model, and it is ensured that it focuses on the relevant area of expertise. The prompt template is presented in Figure 3.

***Few Shots Prompting Application for More Guidance in Operation Examination Task***

With this prompt technique, it is structured to include a few examples input and output pairs to obtain the desired output. Within the framework of this study, a two-example learning approach will be used. As an example, a similar G-Code and the operation type and geometric description of this G-Code will be given. The prompt structure is shown in Figure 4.

***Tree of Thought Prompting Application for Deliberative Reasoning in Operation Examination Task***

With this prompt technique, an attempt has been made to elicit deliberative reasoning for a single interaction with the LLM. Imagining multiple experts encourages the LLM to use various perspectives and generate lines of reason-

***Role:*** *CNC Machine Tool Expert*
***Instruction:*** *Imagine four different experts are analysing this g code, all experts, all experts will write down their own explanation about operation type and geometric description of the corresponding operation, then share it with the group. If any expert realises, they're wrong at any point, then they leave. At the end of this discussion, give the summary of geometric description and operation type via adding experts' conflicts.*
***Input:*** *<GCODE>*
***Explanation:*** *<Area for LLM output>*

**Figure 5**. Tree of thought prompt template for operation examination.

***Role:*** *CNC Machine Tool Expert*
***Instruction:*** *Analyse the below operation and suggest me the suitable tool type, tool material and tool geometry parameters.*
***Input:*** *<Desired machining operation description with geometric explanation and with workpiece material information>*
***Explanation:*** *<Area for LLM output>*

**Figure 6**. Zero shot prompt template for selecting suitable tool properties.

***Role:*** *CNC Machine Tool Expert*
***Instruction:*** *Analyse the below operation and suggest me the suitable tool type, tool material and tool geometry parameters.*
***Example:***
*<Operation Description>,<Tool Type>,<Tool Material>, <Tool Geometry Features>*
***Input :*** *<Desired machining operation description with geometric explanation and with workpiece material information>*
***Explanation :*** *<Area for LLM output>*

**Figure 7**. Few shots prompt template for selecting suitable tool properties.

ing. Each expert sharing their thoughts ensures that these causal steps are clearly expressed. Asking it to realize it is mistaken enables it to perform internal evaluation and eliminate this line of thought. The prompt template is given in Figure 5.

**Prompt Configurations for the Task of Selecting Suitable Tool Properties**

The main purpose at this stage is to evaluate the LLM's ability to recommend suitable cutting tools for a specific Face Milling operation, considering the process requirements and the properties of the workpiece material. Thanks to the relevant prompt, it will be asked to infer information such as "Tool Type" (e.g.: Indexable Face Mill), "Tool Material" (e.g.: Coated Carbide) and "Tool Geometry Features" (e.g.: Diameter, Number of Flute, Length). The properties of the tool will be compared with

***Role:*** *CNC Machine Tool Expert*
***Instruction:*** *Imagine four different experts are analysing this machining operation description, all experts will write down their own explanation about suitable tool type, tool material and tool geometry features, then share it with the group. If any expert realises, they're wrong at any point, then they leave. At the end of this discussion, give the summary of suggested tool type, tool material and tool geometry features via adding experts' conflicts.*
***Input:*** *<Desired machining operation description with geometric explanation and with workpiece material information>*
***Explanation:*** *<Area for LLM output>*

**Figure 8**. Tree of thought prompt template for selecting suitable tool properties.

***Role:*** *CNC Machine Tool Expert*
***Instruction:*** *Analyse the below tool type, tool material and tool geometry, workpiece material, operation type suggest me the suitable Cutting Speed and Feed rate*
***Input:*** *< Desired machining operation type, workpiece material, tool type tool material and tool geometric features.>*
***Explanation:*** *<Area for LLM output>*

**Figure 9**. Zero shot prompt template for spindle speed and feed rate estimation.

applied and used data obtained from factory data as it is mentioned in Section Claude Sonnet v3.7 Evaluation and Section Deepseek-R1 Evaluation.

***Zero Shot Prompting Application for Direct Inference in the Task of Selecting Suitable Tool Properties***

The prompt created using the approach mentioned in Section Claude Sonnet v3.7 is as follows (Fig. 6).

***Few Shots Prompting Application for Deliberative Reasoning in the Task of Selecting Suitable Tool Properties***

The prompt created using the approach mentioned in Section Deepseek-R1 Evaluation is as follows (Fig. 7).

***Tree of Thought Prompting Application for Deliberative Reasoning in the Task of Selecting Suitable Tool Properties***

The prompt created using the approach mentioned in Section GPT4.5 Preview Evaluation is as follows (Fig. 8).

***Prompt Configurations for the Task of Estimating Suitable Spindle Speed and Feed Rate***

The main purpose at this stage is to evaluate the LLM's inference of suitable cutting parameters -cutting speed (RPM) and feed rate (mm/minute)- for a specific workpiece and tool. This allows a direct comparison of model recommendations against reference process values.

***Zero Shot Prompting Application for Direct Inference in the Task of Estimating Suitable Spindle Speed and Feed Rate***

The prompt created using the approach mentioned Section GPT4.5 Preview Evaluation is as follows (Fig. 9).

***Role:*** *CNC Machine Tool Expert*
***Instruction:*** *Analyse the below tool type, tool material and tool geometry, workpiece material, operation type suggest me the suitable Cutting Speed and Feed rate*
***Example:***
*<Workpiece Material>,<Operation Type>,<Tool Type>,<Tool Material>,<Tool Geometry Features>*
***Input:*** *<Desired machining operation type, workpiece material, tool type tool material and tool geometric features>*
***Explanation :*** *<Area for LLM output>*

**Figure 10**. Few shots prompt template for spindle speed and feed rate estimation.

***Few Shots Prompting Application For More Guidance in the Task of Estimating Suitable Spindle Speed and Feed Rate***

The prompt created using the approach mentioned in Section Deepseek-R1 Evaluation Figure is as follows (Fig. 10).

***Tree of Thought Prompting Application for Deliberative Reasoning in the Task of Estimating Suitable Spindle Speed and Feed Tate***

The prompt created using the approach mentioned in Section GPT4.5 Preview Evaluation is as follows (Fig. 11).

## EXPERIMENT AND APPLICATION PROTOCOL

Based on data obtained from the factory environment, sample G-Code blocks will be created with the help of NX CAM. This created G-Code will again be simulated on NX CAM, and the final processed output will be recorded and stored for future comparison [25].

**Application of Prompts**

For each defined prompt – G-Code interpretation, tool selection, and cutting parameter estimation – it will be run on the selected LLM platform. The text-based responses of the LLM will be recorded directly.

**Operation Examination**

The textual description regarding the G Code produced with the help of NX CAM will be evaluated based on known parameters and purpose. The assessment focuses on whether the generated interpretation matches the intended operation and geometry.

**Selecting Tool Properties**

A virtual tool corresponding to the "tool geometry features" suggested by the LLM will be modelled in the simulation environment using the Create MyVirtual Machine application. The "Tool Type" and "Tool Material" outputs will be evaluated by comparing them with data obtained from the factory [26].

**Estimating Spindle Speed and Feed Rate**

The "Cutting Speed" and "Feed Rate" values suggested by the LLM will be applied in the simulation environment using Create MyVirtual Machine application. At this stage,

***Role:*** *CNC Machine Tool Expert*
***Instruction:*** *Imagine four different experts are analysing this desired machining operation type, workpiece material, tool type tool material and tool geometric features, all experts will write down their own explanation about suitable cutting speed and feed rate estimation for given tool, then share it with the group. If any expert realizes, they're wrong at any point, then they leave. At the end of this discussion, give the summary of suggested feed rate and spindle speeds via adding experts' conflicts.*
***Input:*** *<Desired machining operation type, workpiece material, tool type tool material and tool geometric features>*
***Explanation:*** *<Area for LLM output>*

**Figure 11**. Tree of thought prompt template for spindle speed and feed rate estimation.

the tool is virtually modelled in section Face Milling and the G-Code used for interpretation in section Large Language Models will be run.

**Comparison and Verification**

The basic verification control will take place by running the created G-Code in the Create MyVirtual Machine environment. The main criterion for success is "the observation that the processed material is compatible with the NX Cam simulation output.". The properties of the virtually processed part (dimensions of the area where Face Milling is applied) include a geometric comparison of the output provided by NX CAM. The estimation of tool selection and cutting parameters will be verified by comparing them with data obtained from the factory.

**Performance Evaluation Metrics**

A series of metrics will be used to systematically evaluate the performance of LLM outputs throughout different prompt techniques and experimental stages. These metrics are designed by referencing similar academic studies to measure the degree of accuracy and usability of LLM's suggestions [13].

Definition of Success Metrics Related to Operation Examination Task:

- Success: The LLM correctly identifies the operation type and presents an accurate and complete geometric description of the machining features, matching the given G-Code function.
- Partially Success: The LLM correctly identifies the operation type, but the geometric description contains minor deficiencies or errors that do not alter the essence of the operation.
- Unsuccess: The LLM identifies the wrong operation type, or the geometric description is significantly erroneous or misleading.

Definition of Success Metrics Related to Selecting Tool Properties Task:

- Success: All suggested tool parameters ("Tool Type", "Tool Material", "Tool Geometry") represent a valid, optimal, or very close to optimal definition for the relevant machining and workpiece. It will be compared with proven data obtained from the factory.

- Partially Success: The suggested tool is generally suitable but may require minor adjustments for one or more parameters (e.g., if the suggested diameter is close to a standard size) or the suggested tool is a functional alternative, although not optimal.
- Unsuccess: The suggested tool is not suitable for the operation, the material selection is incorrect, or the geometric properties lead to poor performance or failure.

Definition of Success Metrics Related to Estimating Spindle Speed and Feed Rate Task:

- Success: The suggested spindle speed and feed rate values are within an acceptable tolerance range, such as ± 5% of proven values obtained from the factory, and result in smooth machining in the digital twin.
- Partially Success: The parameters are outside the optimal range but do not cause the simulation to fail completely (e.g., longer processing time), the part can still be machined correctly. It remains within the reference value ranges in the datasheet published by the tool manufacturer for the tool used in the factory as it is mentioned in Section Claude Sonnet v3.7 Evaluation and Section Deepseek-R1 Evaluation.
- Unsuccess: The suggested parameters are largely incorrect, leading to errors such as tool breakage, surface defects, or inability to complete the operation. The suggested values are recommended completely independently of the reference ranges in the tool defined factory data as it is mentioned in Section Claude Sonnet v3.7 Evaluation.

## RESULTS AND DISCUSSION

At this stage, the results of the experiments conducted in line with the methodology will be discussed within the following scope. The discussion highlights both strengths and limitations observed across models and prompting techniques.

- Relative strengths and weaknesses of each prompt technique for the selected application specific to the machine tool domain.
- The type of error and tendency to error that LLMs repeat when working with machine tool information.
- The extent to which the current LLM outputs are reliable and the level of modification or expert intervention they generally require.
- Inferences for future research regarding its development for use as a domain assistant.

**Discussions About the Operation Examination Task**

In this section, the operation examination prompts were used for different language models and evaluation results have been discussed. The comparison emphasizes how accurately each model interprets operation type and geometry.

***Claude Sonnet v3.7 Evaluation***

Demonstrated a significant ability in this task. All prompting techniques achieved a "Partially Success" rating.

The Zero Shot model could not identify the operation as "face milling or surface milling", it identified the operation as a "2D profile milling" operation. But the geometrical description was accurate. So, Zero Shot model correctly identified the 4 depth phases of the operation with 0.5 mm of depth. The path start was correctly identified, feed rate has been detected, and the cutting depth of the phases has correctly also identified. What made zero shot model to identify operation not correctly was the circular arcs in the profile shape. It was a face milling operation with smoothing that is why it contained circular arcs. But Zero Shot model detected these as a profile.

The Few Shots model also could not identify this operation as a "face milling or surface milling" operation, it identified the operation as a "Contour Milling operation." But the geometrical description was also accurate. It correctly identified the four depth passes and in which Z coordinates it started. It correctly identified that these passes have the same pattern, and this operation is a high-precision operation with high-precision compression mode. It also detected that there is smooth motion control.

The Tree of Thought approach, leveraging simulated expert consensus, also could not identify the operation as "Face milling / Surface machining." The geometric description mirrored Zero-Shot's accuracy in most aspects, including the same minor X-limit discrepancy.

***Deepseek-R1 Evaluation***

Demonstrated a medium rated ability for this task. All prompting techniques could determine geometric descriptions but had failure determining the operation.

The Zero Shot prompting model has detected the operation as "2.5D Milling". It correctly identified the 4 passes at correct depths. It could also identify the feed rate and spindle speed from the given g-code and could describe the contouring path correctly.

The Few Shots model also could not identify this operation as a "face milling or surface milling" operation, it identified the operation as a "Contour Milling" operation. But the geometrical description was also accurate. It correctly identified that there exists multiple depth passes and in which Z coordinates it started. It correctly identified that these passes have the same pattern. It correctly identified that the operation uses step-down milling with positional accuracy tolerances of 0.01 mm on all axes.

Tree of Thoughts approach has determined the operation type as "3-axis symmetrical profile finishing". The multilevel passes were in the expert discussion, but it was not included in the conclusion. The interpolation turning and linear movements were also included in the expert discussion, but it was not declared in conclusion. There was no information about spindle speed or feed rate.

***GPT4.5 Preview Evaluation***

Demonstrated a medium rate of ability with whole types of prompting. It could be said that GPT4.5 was not generally successful for this type of domain.

The Zero Shot model has determined the given operation as a "contour milling" operation. It could deter-

mine that there exists a there are contour passes from 5 to 0, but the accurate path or a step depth was not determined. The feed rate and spindle speed were also found from operation.

The Few Shots model had determined the operation as a "pocket milling" operation. It has been determined that the operation starts with an approach to 5 mm in Z and proceeds with cutting in different depths. The depths steps were given correctly. The spindle speed and feed rate were present. It also included there exists smooth transitions between segments with features like radii of 7.281 mm.

Tree of Thoughts approach generally failed. It determined the operation as a "roughing operation" with an end mill tool. The operation was made with a facing tool. The steps were also determined in the summary and discussion.

**Comparison Between Language Models**

With every prompt technique; all language models have failed to determine the operation type. They successfully found the depth step passes and determined the machining parameters that are contained in the operation. Geometrical descriptions were present, but did not cover the whole operation details. It would really need additional comments and information from operators to achieve more.

The best answers were provided from Claude V3.7 Sonnet. Other than operation classification, geometrical descriptions of the Claude V3.7 Sonnet were more detailed and more accurate. The summary of evaluation results is presented in Table 1.

**Discussions About the Selecting Tool Properties Task**

***Claude Sonnet v3.7 Evaluation***

All evaluated prompting techniques achieved a "Partially Success" rating. This indicates a general suitability of the suggestions, though none perfectly matched GT's specific optimal tool.

In Zero Shots, the model correctly recommended a "Face mill cutter with multiple inserts " with material "Coated carbide inserts," which aligns with the GT and workpiece material. For tool geometry parameters, the model suggested a diameter range of 63-80 mm for this operation but has not determined a specific diameter as in ground truth. The number of flutes is also not specified, but a range of 5-8 has been given as a suggestion via model. Cutting angle was specified as 45 °. This was also a tool information that is determined in ground truth.

Few Shots approach also correctly identified the "Facing Tool" type and "Carbide with TiAlN coating." It suggested specific parameters: L=80mm (GT: 100mm), D=63mm (GT: 25mm), and 5 Flutes (GT: 3). While the diameter differed, 63 mm is a standard and functional alternative.

The Tree of Thought summary correctly identified the "Face mill cutter" type and a consensus on "carbide inserts." The geometric discussion was rich, mentioning positive rake angles and lead angles. However, the final summary did not converge on specific dimensions for diameter or flute count matching the GT, instead offering characteristics of a suitable tool class.

**Table 1.** Operation examination results for selected LLMs

| LLMs | Success | Partially success | Unsuccess |
|---|---|---|---|
| Claude v3.7 sonnet | | * | |
| Deepseek-R1 | | | * |
| GPT 4.5 | | | * |

***Deepseek-R1 Evaluation***

With this model, the few shots prompting technique achieved a "Partially Success" rating. Other techniques have not been so successful for suggesting an alternative functional tool or a similarity with ground truth. This indicates a general suitability of the suggestions, though none perfectly matched GT's specific optimal tool.

With Zero Shot approach, the model correctly recommended a "Face milling tool with indexable inserts". The material was "Carbide with TiAlN coating. It suggested s 4-6 numbers of flutes but did not suggest a diameter. It specified a 45 ° lead angle, positive rake angle. There were no diameters or tool length specified. It can be said that a base shape for a cutter has been determined but specified alternative or a ground truth-based example has not been given.

With Few Shots approach, the parameters were specified. It correctly identified the operation as a face milling and gave a suggestion for the tool type as "face milling cutter" with material as" carbide with TiAlN coating". It gave tool length 80 mm (GT: 100 mm), diameter as 63 mm (GT: 25 mm), number of flutes as 5 (GT: 3). This correctly establishes a functional alternative for the operation as a suggestion.

With the Tree of Thoughts approach, the parameters were not specified in the Summary. It correctly identified the operation as a face milling and gave a suggestion for the tool type as "face milling cutter" with material as" carbide with TiAlN coating". The model did not suggest a diameter, number of flute or tool length. No similarity or ground truth has been determined by model for this operation with this prompting approach.

***ChatGPT-4.5 Preview Evaluation***

With ChatGPT-4.5 Preview model, the few shots prompting technique achieved a "Partially Success" rating. Other techniques were not suitable for suggesting an alternative functional tool or a similarity with ground truth. This indicates a general suitability of the suggestions, though none perfectly matched GT's specific optimal tool.

In Zero Shot approach, the model correctly recommended a "Face milling tool with indexable inserts". The material was "Carbide with TiAlN coating. No specific parameters for length, diameter or number of flutes have been suggested. It specified a 45 ° lead angle, positive rake angle.

In Few Shots approach, the parameters were specified. It correctly identified the operation as a face milling and gave a suggestion for the tool type as "facing tool" with material as" carbide ISO P-type recommended". It gave tool length 80 mm (GT: 100 mm), diameter as 50 mm (GT: 25 mm), number of flutes as 4 (GT: 3). This correctly establishes a functional alternative for the operation as a suggestion.

**Table 2.** Selecting tool properties results for selected LLMs

| LLMs | Success | Partially success | Unsuccess |
|---|---|---|---|
| Claude v3.7 Sonnet | | * | |
| Deepseek-R1 | | * | |
| GPT 4.5 | | * | |

In the Tree of Thoughts approach, the parameters were not specified in the Summary. It correctly identified the operation as a face milling and gave a suggestion for the tool type as “face milling cutter” with material as” carbide with TiAlN coating”. The model did not suggest a diameter, number of flute or tool length. No similarity or ground truth has been determined by model for this operation with this prompting approach.

**Comparison Between Language Models**

The Few-Shots approach established good reasoning with different models; however, apart from this approach, the information provided was insufficient to create a functional alternative tool or a similar tool with ground truth. The best scenario was established by Claude V.37 Sonnet. The evaluation results are summarized in Table 2.

**Discussions about the Estimating Spindle Speed and Feed Rate Task**

***Claude Sonnet v3.7 Evaluation***

With the Zero Shot technique, parameters derived (n=2292 RPM, Vf=1032 mm/min) based on standard machining parameters (Vc = 180 m/min, fz = 0.15 mm/tooth). While these are common catalogue values for C40 steel with carbide and would likely allow the operation to proceed without immediate tool failure, the given suggestion and actual GT values differ. The federate for finishing in GT was approximately 10 times lower than the suggested feed rate. Spindle speed for this operation has been suggested by model also approximately 4 times bigger than the GT. This significant discrepancy renders the output "Unsuccess" when compared against the factory's proven, high-performance values. Its relative "strength" (if any in this context) was adherence to general safe practices, but this was insufficient for the task's success criteria.

With the Few Shots technique, parameters derived (n=2000 RPM, Vf=900 mm/min) based on standard machining parameters (Vc = 160 m/min, fz = 0.15 mm/tooth). While these are common catalogue values for C40 steel with carbide and would likely allow the operation to proceed without immediate tool failure, the given suggestion and actual GT values differ. The federate for finishing in GT was approximately 8 times lower than the suggested feed rate. Spindle speed for this operation has been suggested by model also approximately 4 times bigger than the GT. This significant discrepancy renders the output "Unsuccess" when compared against the factory's proven, high-performance values. Its relative "strength" (if any in this context) was adherence to general safe practices, but this was insufficient for the task's success criteria.

The Tree of Thought's consolidated recommendations (n=2230 RPM, Vf=1000 mm/min) were, like Zero-Shot, based on conservative, widely accepted cutting speeds (Vc≈207 m/min) and feeds per tooth (fz≈0.12 mm/tooth). These deviated from the GT by approximately 3 times greater and 10 times greater. While the reasoning process involved simulated expert discussion, the outcome still fell far bigger of GT’s optimized parameters, leading to an "Unsuccess" rating.

***Deepseek-R1 Evaluation***

With the Zero Shot technique, parameters derived (n=2546 RPM, Vf=1500 mm/min) based on standard machining parameters (Vc = 200 m/min, fz = 0.2 mm/tooth). While these are common catalogue values for C40 steel with carbide and would likely allow the operation to proceed without immediate tool failure, the given suggestion and actual GT values differ. The federate for finishing in GT was approximately 10 times lower than the suggested feed rate. Spindle speed for this operation has been suggested by model also approximately 4 times bigger than the GT. This significant discrepancy renders the output "Unsuccess" when compared against the factory's proven, high-performance values. Its relative "strength" (if any in this context) was adherence to general safe practices, but this was insufficient for the task's success criteria.

With the Few Shots technique, parameters derived (n=2000 RPM, Vf=900 mm/min) based on standard machining parameters (Vc = 160 m/min, fz = 0.15 mm/tooth). While these are common catalogue values for C40 steel with carbide and would likely allow the operation to proceed without immediate tool failure, the given suggestion and actual GT values differ. The federate for finishing in GT was approximately 8 times lower than the suggested feed rate. Spindle speed for this operation has been suggested by model also approximately 4 times bigger than the GT. This significant discrepancy renders the output "Unsuccess" when compared against the factory's proven, high-performance values. Its relative "strength" (if any in this context) was adherence to general safe practices, but this was insufficient for the task's success criteria.

The Tree of Thought's consolidated recommendations (n=1900 RPM, Vf=750 mm/min) were, like Zero-Shot, based on conservative, widely accepted cutting speeds (Vc≈207 m/min) and feeds per tooth (fz≈0.12 mm/tooth). These deviated from the GT by approximately 3 times greater for spindle speed and 7 times greater for feed rate. While the reasoning process involved simulated expert discussion, the outcome still fell far bigger of GT’s optimized parameters, leading to an "Unsuccess" rating.

***ChatGPT-4.5 Preview Evaluation***

With the Zero Shot technique, parameters derived (n=2290 RPM, Vf=680 mm/min) based on standard machining parameters (Vc = 180 m/min, fz = 0.15 mm/tooth). The suggestion given and actual GT values differ. The federate for finishing in GT was approximately 5 times lower than the suggested feed rate. Spindle speed for this operation has been suggested by model also approximately 3 times bigger than the GT. This significant discrepancy renders the out-

**Table 3.** Estimating spindle speed and feed rate results for selected LLMs

| LLMs | Success | Partially success | Unsuccess |
|---|---|---|---|
| Claude v3.7 Sonnet | | | * |
| Deepseek-R1 | | | * |
| GPT 4.5 | | | * |

put "Unsuccess" when compared against the factory's proven, high-performance values. Its relative "strength" (if any in this context) was adherence to general safe practices, but this was insufficient for the task's success criteria.

With the Few Shots technique, parameters derived (n=2040 RPM, Vf=920 mm/min) based on standard machining parameters (Vc = 140 m/min, fz = 0.15 mm/tooth). While these are common catalogue values for C40 steel with carbide and would likely allow the operation to proceed without immediate tool failure, the given suggestion and actual GT values differ. The federate for finishing in GT was approximately 8 times lower than the suggested feed rate. Spindle speed for this operation has been suggested by model also approximately 4 times bigger than the GT. This significant discrepancy renders the output "Unsuccess" when compared against the factory's proven, high-performance values. Its relative "strength" (if any in this context) was adherence to general safe practices, but this was insufficient for the task's success criteria.

The Tree of Thought's consolidated recommendations (n=1700 RPM, Vf=1000 mm/min) were, like Zero-Shot, based on conservative, widely accepted cutting speeds (Vc≈135 m/min) and feeds per tooth (fz≈0.2 mm/tooth). These deviated from the GT by approximately 3 times greater for spindle speed and 10 times greater for feed rate. While the reasoning process involved simulated expert discussion, the outcome still fell far bigger of GT's optimized parameters, leading to an "Unsuccess" rating.

**Comparison Between Language Models**

The ground truth values differ a lot with the suggested values with all language models. Spindle speed values were much higher than ground truth for every model, it was also the same for feed rate. It can be said that standard values for calculation of the feed rate and spindle speed are not enough to get optimum cutting speeds. The results are presented in Table 3.

## CONCLUSION

This study evaluated three foundational large language models — Claude V3.7 Sonnet, DeepSeek-R1, and GPT-4.5 — across three core machining tasks (operation examination, cutting-tool selection, and spindle-speed / feed-rate estimation) using zero-shot, few-shot, and tree-of-thought prompting. The outputs were verified against industry-standard CAM software (Siemens NX [25]) and digital twin simulations (Create MyVirtual Machine [26]). The results reveal a clear gradient of capability: LLMs can partially interpret machining operations, can propose functional alternative cutting tools under guided prompting, but consistently fail at quantitative parameter estimation — with suggested spindle speeds and feed rates deviating from factory-proven values by factors of three to ten.

A central finding is that apparent improvements in LLM output can mask underlying safety hazards — a pattern appropriately described as "false efficiency." Campean and Pop [30] independently demonstrated this phenomenon: ChatGPT's optimization of a CNC milling program yielded a 37 % cycle-time reduction, yet 83 % of that saving resulted from the silent deletion of a required pocket-milling operation and the removal of safety-critical G43 and G28 commands, producing a non-conforming part. In the present study, the 3–10× parameter overestimates would likewise shorten nominal cycle times while simultaneously pushing the process into regimes that risk tool breakage, workpiece scrap, and machine collision. These results caution against interpreting raw LLM-generated metrics as genuine process improvements without rigorous physical verification.

The experiments further demonstrate that deploying LLMs in the machining domain does not eliminate the need for human expertise — it redistributes it. Every LLM output in this study required expert review: operation descriptions needed correction of misidentified operation types, tool suggestions required dimensional adjustment, and parameter estimates had to be discarded entirely. Rather than reducing the operator's cognitive load, the current generation of LLMs shifts the burden from direct task execution to output verification — a distinction that must be acknowledged when assessing the practical value proposition of LLM-assisted manufacturing. Aghaei and Ansari [31] reached a similar conclusion in their broad review, noting that foundation language models generate linguistically plausible but technically inaccurate answers and that safety-critical validation mechanisms are rarely integrated into existing workflows.

Importantly, the failures observed in parameter estimation cannot be attributed solely to prompt engineering deficiencies. Even the tree-of-thought technique — which structures multi-step deliberative reasoning and represents the most sophisticated prompting strategy tested — produced "Unsuccess" results across all three models. This outcome indicates that the limitation is not in how questions are posed to the model but in the model's fundamental lack of deterministic, physics-grounded reasoning. LLMs generate outputs by statistical next-token prediction over textual corpora; they do not solve the underlying force-balance, thermal, and vibration equations that govern metal-cutting dynamics. Consequently, no refinement of natural-language prompting alone is likely to bridge the gap between catalogue-level heuristics and the process-specific parameter sets that safe, efficient machining demands.

Given this structural limitation, future research should explore hybrid architectures that combine the natural-language interface strengths of LLMs with physics-informed computational methods. Physics-informed neural networks (PINNs) have recently demonstrated the ability to encode governing equations directly into the learning process for machining applications. Darshan et al. [32] developed a physics-informed cutting-force model for end milling that

achieved high predictive accuracy with limited experimental data by embedding force-equilibrium constraints into the network loss function. Zhang et al. [33] proposed a hierarchical Bayesian PINN for the inverse estimation of grinding process parameters grounded in contact-mechanics theory. These advances suggest that coupling an LLM front-end — responsible for G-code interpretation, intent parsing, and report generation — with a PINN back-end — responsible for physics-constrained parameter estimation and process simulation — could yield a system that retains the accessibility of natural-language interaction while delivering the quantitative reliability that standalone LLMs currently lack.

In summary, while foundational LLMs represent a promising interface technology for the machine tool domain, the present results demonstrate that they are not yet a substitute for domain expertise in safety-critical machining decisions. Their deployment should be accompanied by mandatory verification through digital twin simulation and expert oversight, and future development should focus on integrating physics-based reasoning capabilities rather than relying solely on larger training corpora or more elaborate prompting strategies.

**Data Availability Statement**

The authors confirm that the data that supports the findings of this study are available within the article. Raw data that support the finding of this study are available from the corresponding author, upon reasonable request.

**Author's Contributions**

Ugur Eniş: Conception, Design, Methodology, Data Collection and Processing, Prompt Engineering, LLM Evaluation, Analysis and Interpretation, Literature Review, Writer, Critical Review, GitHub Repository Management.

Mehmet Şamil Soyer: Conception, Design, Virtual Twin Simulation, CAM Software Verification, Data Processing, Analysis and Interpretation, Literature Review, Writer, Critical Review.

Hanife Ünal Helvacıoğlu: Conception, Supervision, Methodology Design, Analysis and Interpretation, Literature Review, Critical Review.

Muhammet Mustafa Savasçı: Conception, Supervision, Methodology Design, Analysis and Interpretation, Literature Review, Critical Review.

**Conflict of Interest**

The authors declared no potential conflicts of interest with respect to the research, authorship, and/or publication of this article.

**Statement on the Use of Artificial Intelligence**

This research evaluates the capabilities of large language models (LLMs) including Claude v3.7 Sonnet, DeepSeek-R1, and GPT-4.5 for machining parameter estimation and G-code interpretation. These AI models were the subject of the study, not tools used in writing the manuscript. The manuscript itself was written by the authors without the assistance of generative AI writing tools.

**Ethics**

There are no ethical issues with the publication of this manuscript.

## REFERENCES


[1] Parashar, B. S. N., & Mittal, R. (2013). *Elements of manufacturing processes*. PHI Learning Pvt. Ltd.

[2] Yusup, N., Zain, A. M., & Hashim, S. Z. M. (2012). Evolutionary techniques in optimizing machining parameters: Review and recent applications (2007-2011). *Expert Systems with Applications, 39*, 9909-9927. [CroosRef]

[3] Davis, J. R. (Ed.). (1989). *ASM handbook, volume 16: Machining*. ASM International.

[4] Soori, M., Arezoo, B., & Dastres, R. (2023). Machine learning and artificial intelligence in CNC machine tools, a review. *Sustainable Manufacturing and Service Economics, 2*, Article 100014. [CroosRef]

[5] Pimenov, D. Y., Bustillo, A., Wojciechowski, S., Sharma, V. S., Gupta, M. K., & Kuntoğlu, M. (2023). Artificial intelligence systems for tool condition monitoring in machining: Analysis and critical review. *Journal of Intelligent Manufacturing, 34*, 2079-2121. [CroosRef]

[6] Navaneethan, G., Palanisamy, S., Jayaraman, P. P., Kang, Y.B., Stephens, G., Papageourgiou, A., & Navarro-Devia, J. (2024). A review of automated cutting tool selection methods. *The International Journal of Advanced Manufacturing Technology, 133*, 1063-1092. [CroosRef]

[7] Oberg, E., Jones, F. D., Horton, H. L., Ryffel, H. H., & McCauley, C. J. (2020). *Machinery's handbook* (31st ed.). Industrial Press.

[8] Li, Y., Zhao, H., Jiang, H., Pan, Y., Liu, Z., Wu, Z., Shu, P., Tian, J., Lyu, Y., Blenk, P., Pence, J., Rupram, J., Banu, E., Liu, N, Song, W., Zhai, X., Song, K., Zhu, D., Li, B., Wang, X., & Liu, T. (2024). Large language models for manufacturing. *arXiv*. Preprint. doi: 10.48550/arXiv.2410.21418

[9] Makatura, L., Foshey, M., Wang, B., Hähnlein, F., Ma, P., Deng, B., Tjandrasuwita, M., Spielberg, A., Owens, C. E., Chen, P. Y., Zhao, A., Zhu, A., Norton, W. J., Gu, E., Jacob, J., Li, Y., Schulz, A., & Matusik, W. (2024). *Large language models for design and manufacturing*. MIT GenAI. https://mit-genai.pubpub.org/pub/nmypmnhs Accessed Jun 03, 2026. [CroosRef]

[10] Ni, M., Wang, T., Leng, J., Chen, C., & Chen, L. (2025). A large language model-based manufacturing process planning approach under industry 5.0. *International Journal of Production Research*, 1-20. [CroosRef]

[11] Shahin, M., Hosseinzadeh, A., & Chen, F. F. (2025). Generative artificial intelligence in manufacturing: Applications, case studies, and future directions for next-generation intelligent production systems. The *International Journal of Advanced Manufacturing Technology, 141*(3-4), 1159-1265. [CroosRef]

[12] Mata, O., Ponce, P., Perez, C., & Ramirez, M. (2026). Digital twin designs with generative AI: Crafting a comprehensive framework for manufacturing systems. *Journal of Intelligent Manufacturing, 37*, 1049-1072. [CroosRef]

[13] Jignasu, A., Marshall, K., Ganapathysubramanian, B., Balu, A., Hegde, C., & Krishnamurthy, A. (2023). Towards foundational AI models for additive manufacturing: Language models for G-code debugging, manipulation, and comprehension. *arXiv*. Preprint. doi: 10.48550/arXiv.2309.02465 [CroosRef]

[14] Šket, K., Potočnik, D., Brezočnik, M., & Ficko, M. (2025). Large language models for G-code generation in CNC machining: A comparison of ChatGPT-3.5 and ChatGPT-4o. *Advances in Production Engineering & Management, 20*(2), 224-238. [CroosRef]

[15] Abdelaal, M., Lokadjaja, S., & Engert, G. (2025). GLLM: Self-corrective G-code generation using large language models with user feedback. *arXiv*. Preprint. doi: 10.48550/arXiv.2501.17584

[16] Kanimozhi, S., & Sriker, Y. S. (2024). Explorative deployment of fine-tuned large language model for on-site computerized numeric control machine operator assistance. *2024 IEEE Silchar Subsection Conference (SILCON)*. IEEE.

[17] Jeon, J., Sim, Y., Lee, H., Han, C., Yun, D., & Kim, E. (2026). CNC-talks: Conversational machine monitoring via large language model and real-time data retrieval augmented generation. *Journal of Manufacturing Systems, 85*, 678-688. [CroosRef]

[18] Stathatos, E., Benardos, P., & Vosniakos, G. C. (2026). Large language models for high-level computer-aided process planning in a distributed manufacturing paradigm. *Robotics and Computer-Integrated Manufacturing, 100*, 103233. [CroosRef]

[19] Smid, P. (2003). *CNC programming handbook: A comprehensive guide to practical CNC programming*. Industrial Press.

[20] Stephenson, D. A., & Agapiou, J. S. (2016). *Metal cutting theory and practice* (3rd ed.). CRC Press. [CroosRef]

[21] Ouyang, L., Wu, J., Jiang, X., Almeida, D., Wainwright, C. L., Mishkin, P., Zhang, C., Agarwal, S., Slama, A., Schulman, J., Hilton, J., Kelton, F., Miller, K., Simens, M., Askell, A., Welinder, P., Christiano, P., Leike, J., & Lowe, R. (2022). Training language models to follow instructions with human feedback. *arXiv*. Preprint. doi: 10.48550/arXiv.2203.02155

[22] Wei, J., Bosma, M., Zhao, V. Y., Guu, K., Yu, A. W., Lester, B., Du, N., Dai, A. M., & Le, Q. V. (2021). Finetuned language models are zero-shot learners. *arXiv*. Preprint. doi: 10.48550/arXiv.2109.01652

[23] Min S, Lyu X, Holtzman A, Artetxe M, Lewis M, Hajishirzi H, & Zettlemoyer, L. Rethinking the role of demonstrations: What makes in-context learning work? *arXiv*. Preprint. doi: 10.48550/arXiv.2202.12837

[24] Wei, J., Wang, X., Schuurmans, D., Bosma, M., Ichter, B., Xia, F., Chi, E., Le, Q., & Zhou, D. (2022). Chain-of-thought prompting elicits reasoning in large language models. *arXiv*. Preprint. doi: 10.48550/arXiv.2201.11903

[25] Siemens Digital Industries Software. (n.d.). *NX CAM software: NX for manufacturing*. Siemens Digital Industries Software. https://www.siemens.com/en-us/products/nx-manufacturing/cam-software Accessed on Jun 03, 2026.

[26] Siemens AG. (n.d.). *Run MyVirtual Machine. Retrieved 2024, from Siemens AG*. https://www.dex.siemens.com/industrialsoftware/machine-tool-software/create-myvirtual-machine-operate Accessed on Jun 03, 2026.

[27] Anthropic. (2025, February 24). *Claude 3.5 Sonnet*. https://www.anthropic.com/news/claude-3-7-sonnet Accessed on Jun 03, 2026

[28] DeepSeek. (2025, January 20). *DeepSeek-R1*. https://api-docs.deepseek.com/news/news250120 Accessed on Jun 03, 2026

[29] OpenAI. (2025, February 27). *GPT 4.5*. https://openai.com/index/introducing-gpt-4-5 Accessed on Jun 03, 2026

[30] Campean, E., & Pop, G. (2026). CNC milling optimization via intelligent algorithms: An AI-based methodology. *Machines, 14*(1), 89. [CroosRef]

[31] Aghaei, S., & Ansari, F. (2026). Foundation language models through the lens of manufacturing. *Production & Manufacturing Research, 14*(1), 2632468. [CroosRef]

[32] Darshan, S., Desai, K. A., & Bhattacharyya, A. (2025). Physics-informed experimental design for neural network-based cutting force model in end milling of carbon fiber reinforced polymer composites. *Journal of Manufacturing Processes, 42*, 440-452. [CroosRef]

[33] Zhang, Q., Zhang, Q., Zhao, Y., Liu, Y., Wang, Z., & Ma, Y. (2025). Inverse solution of process parameters in gear grinding using hierarchical Bayesian physics informed neural network (HBPINN). *Scientific Reports, 15*, 18005. [CroosRef]